

Structures and Conformational Dynamics of Gold(I) Halide Complexes of Resorcinarene Tetrakisphosphinite Ligands

Dana J. Eisler and Richard J. Puddephatt*

Department of Chemistry, University of Western Ontario, London, Canada N6A 5B7

Received April 23, 2003

Gold(I) halide derivatives of several tetrakis(diphenylphosphinite) tetraester resorcinarene compounds have been prepared. The complexes are shown to exist in boat conformations, and two different boat conformations were characterized by X-ray structure determinations; the structural characterization of both boat conformations of the same parent resorcinarene is unprecedented. Intramolecular Au••Au interactions were observed in the solid state for both boat conformers and could cause twisting of the resorcinarene skeleton. Several of the complexes exist in solution as an equilibrium mixture of the two different boat conformers, and the equilibrium and dynamics of exchange were studied by variable-temperature NMR.

Introduction

The chemistry of gold(I) coordination compounds has developed rapidly,^{1–9} with the tendency for linear coordination with secondary aurophilic interactions, giving it a

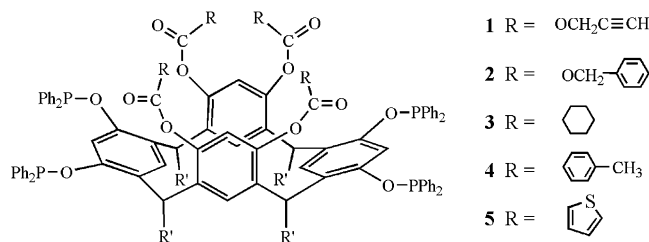
distinctive character.² The secondary intermolecular Au••Au interactions can give supramolecular association to form dimers, oligomers, or even polymers,^{1–3} provided that bulky ligands do not prevent close approach.⁴ Intramolecular Au••Au interactions are also observed for complexes in which two or more gold(I) centers are present.⁵ While gold(I) tends to form linear two-coordinate complexes, it is well established that three- and four-coordinate gold(I) complexes can be formed.⁸

This article reports gold(I) complexes of a series of tetrakisphosphinite resorcinarene compounds, **1–5**, which tend to adopt a boat conformation as shown in Chart 1.¹⁰ The ligands are expected to form four PAuX units (X = anion such as halide) by complexation through the four phosphorus

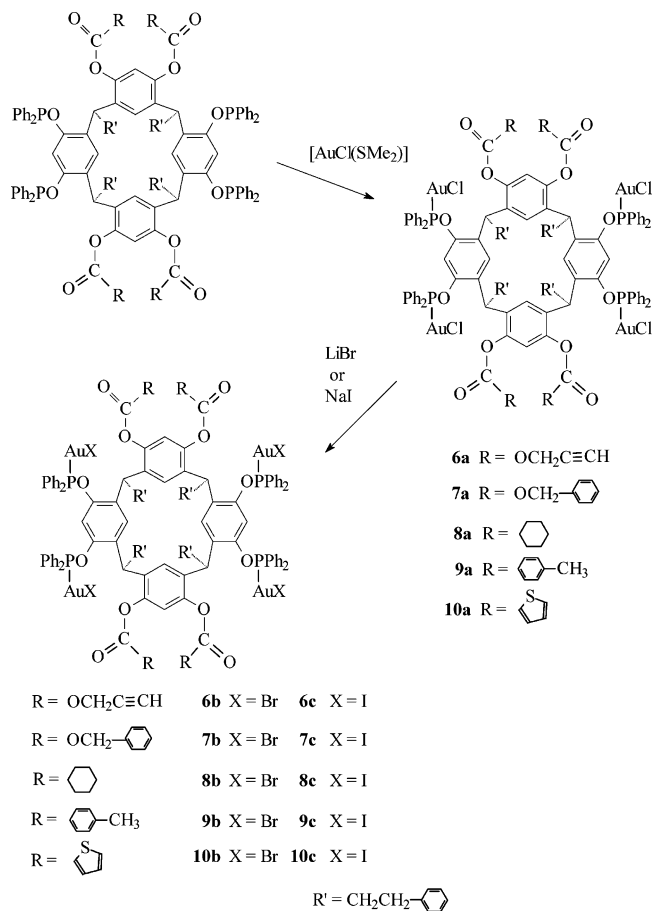
* To whom correspondence should be addressed. E-mail: pudd@uwo.ca. Fax: (519)661-3022.

- (1) (a) Fackler, J. P. *Inorg. Chem.* **2002**, *41*, 6959. (b) Schwerdtfeger, P.; Hermann, H. L.; Schmidbaur, H. *Inorg. Chem.* **2003**, *42*, 1334. (c) Lee, Y. A.; McGarrah, J. E.; Lachicotte, R. J.; Eisenberg, R. *J. Am. Chem. Soc.* **2002**, *124*, 10662. (d) White-Morris, R. L.; Olmstead, M. M.; Balch, A. L. *J. Am. Chem. Soc.* **2003**, *125*, 1033.
- (2) (a) Pathaneni, S. S.; Desiraju, G. R. *J. Chem. Soc., Dalton Trans.* **1993**, 319. (b) Schmidbaur, H. *Chem. Soc. Rev.* **1995**, 319. (c) Pyykkö, P. *Chem. Rev.* **1997**, *97*, 597.
- (3) (a) Puddephatt, R. J. *Chem. Commun.* **1998**, 1055. (b) Irwin, M. J.; Manojlovic-Muir, L.; Muir, K. W.; Puddephatt, R. J.; Yufit, D. S. *Chem. Commun.* **1997**, 219. (c) Angermaier, K.; Zeller, E.; Schmidbaur, H. *J. Organomet. Chem.* **1994**, *472*, 371. (d) Leznoff, D. B.; Xue, B.-Y.; Batchelor, R. J.; Einstein, F. W. B.; Patrick, B. O. *Inorg. Chem.* **2001**, *40*, 6026. (e) Balch, A. L.; Fung, E. Y.; Olmstead, M. M. *J. Am. Chem. Soc.* **1990**, *112*, 5181. (f) Bennett, M. A.; Bhargava, S. K.; Griffiths, K. D.; Robertson, G. B. *Angew. Chem., Int. Ed. Engl.* **1987**, *26*, 260. (g) Irwin, M. J.; Jia, G.; Payne, N. C.; Puddephatt, R. *J. Organometallics* **1996**, *15*, 51. (h) MacDonald, M.-A.; Puddephatt, R. *J. Organometallics* **2000**, *19*, 2194. (i) Irwin, M. J.; Vittal, J. J.; Puddephatt, R. *J. Organometallics* **1997**, *16*, 3541. (j) Attar, S.; Bearden, W. H.; Alcock, N. W.; Alyea, E. C.; Nelson, J. H. *Inorg. Chem.* **1990**, *29*, 425. (k) Dieleman, C. B.; Matt, D.; Neda, I.; Schmutzler, R.; Thönnessen, H.; Jones, P. G.; Harriman, A. *J. Chem. Soc., Dalton Trans.* **1998**, 2115.
- (4) (a) Barron, P. F.; Engelhardt, L. M.; Healy, P. C.; Oddy, J.; White, A. H. *Aust. J. Chem.* **1987**, *40*, 1545. (b) Bott, R. C.; Bowmaker, G. A.; Buckley, R. W.; Healy, P. C.; Perara, M. C. S. *Aust. J. Chem.* **1999**, *52*, 271.
- (5) (a) Xiao, H.; Weng, Y.-X.; Wong, W.-T.; Mak, T. C. W.; Che, C.-M. *J. Chem. Soc., Dalton Trans.* **1997**, 221. (b) Schmidbaur, H.; Graf, W.; Müller, G. *Angew. Chem., Int. Ed. Engl.* **1988**, *27*, 417. (c) Stützer, A.; Bissinger, P.; Schmidbaur, H. *Chem. Ber.* **1992**, *125*, 367. (d) Schmidbaur, H.; Wohlleben, A.; Wagner, F.; Orama, O.; Huttner, G. *Chem. Ber.* **1977**, *110*, 1748.
- (6) Pyykkö, P.; Li, J.; Runeberg, N. *Chem. Phys. Lett.* **1994**, *218*, 133.
- (7) (a) Toronto, D. V.; Weissbart, B.; Tinti, D. S.; Balch, A. L. *Inorg. Chem.* **1996**, *35*, 2484. (b) Van Calcar, P. M.; Olmstead, M. M.; Balch, A. L. *Inorg. Chem.* **1997**, *36*, 5231. (c) Assefa, Z.; McBurnett, B. G.; Staples, R. J.; Fackler, J. P., Jr.; Assmann, B.; Angermaier, K.; Schmidbaur, H. *Inorg. Chem.* **1995**, *34*, 75.
- (8) (a) Gimeno, M. C.; Laguna, A. *Chem. Rev.* **1997**, *97*, 511. (b) Brandys, M.-C.; Puddephatt, R. J. *J. Am. Chem. Soc.* **2001**, *123*, 4839. (c) Jones, P. G.; Sheldrick, G. M.; Muir, J. A.; Muir, M. M.; Pulgar, L. B. *J. Chem. Soc., Dalton Trans.* **1982**, 2123. (d) Dieleman, C. B.; Matt, D.; Harriman, A. *Eur. J. Inorg. Chem.* **2000**, 831.
- (9) (a) Puszta, S. V.; Wei, A.; Stavens, K. B.; Andres, R. P. *Supramol. Chem.* **2002**, *14*, 291. (b) Friggeri, A.; van Veggel, F. C. J. M.; Reinhoudt, D. N. *Chem.—Eur. J.* **1999**, *5*, 3595. (c) Nabeshima, T.; Saiki, T.; Sumitomo, K. *Org. Lett.* **2002**, *4*, 3207. (d) Baaden, M.; Wipff, G.; Yafian, M. R.; Burgard, M.; Matt, D. *J. Chem. Soc., Perkin Trans.* **2000**, *2*, 1315. (e) Lukin, O.; Vysotsky, M. O.; Kalchenko, V. I. *J. Phys. Org. Chem.* **2001**, *14*, 468.
- (10) (a) Eisler, D. J.; Puddephatt, R. J. *Can. J. Chem.*, in press. (b) Tamaki, A.; Kochi, J. K. *J. Organomet. Chem.* **1974**, *64*, 411. (c) Brandys, M.-C.; Jennings, M. C.; Puddephatt, R. J. *J. Chem. Soc., Dalton Trans.* **2000**, 4601.

Chart 1. Tetrakis(diphenylphosphinito)resorcinarene Compounds



Scheme 1

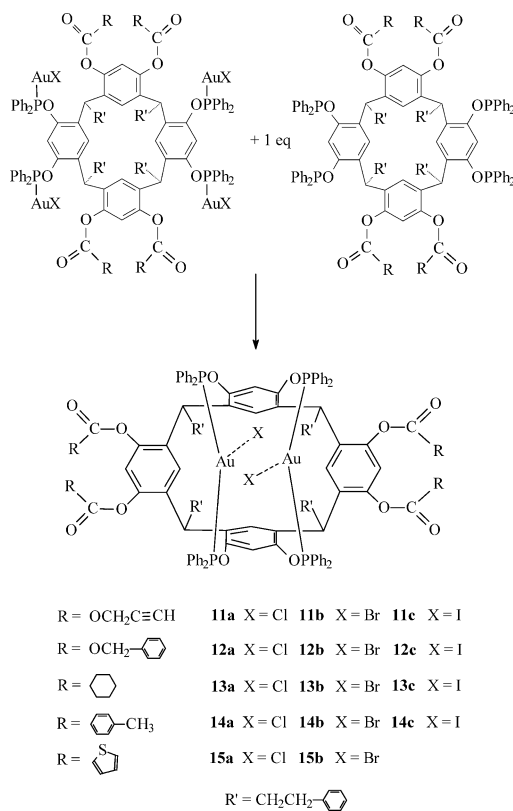


donors. The ligand architecture should then lead to interesting gold(I) coordination complexes, because formation of intramolecular $\text{Au}\cdots\text{Au}$ interactions could profoundly affect the conformation of the resorcinarene skeleton while intermolecular aurophilic attractions could lead to formation of dimers, oligomers, or polymers. The steric and electronic effects of the “spectator” groups R (Chart 1) can be modified easily (examples of carboxylate and carbonate esters are reported), and so a systematic study of the conformations as a function of substituents is possible. It is important to understand the conformational properties because potential applications in sensors or in catalysis rely on the selective inclusion of guest molecules, on the basis of their size and shape, by the resorcinarene host.⁹

Results and Discussion

Synthesis of the Gold(I) Resorcinarene Complexes. The new gold(I) complexes **6–10** (Scheme 1) were prepared by reaction of $[\text{AuCl}(\text{SMe}_2)]^{10}$ with the tetraphosphinite ligands

Scheme 2



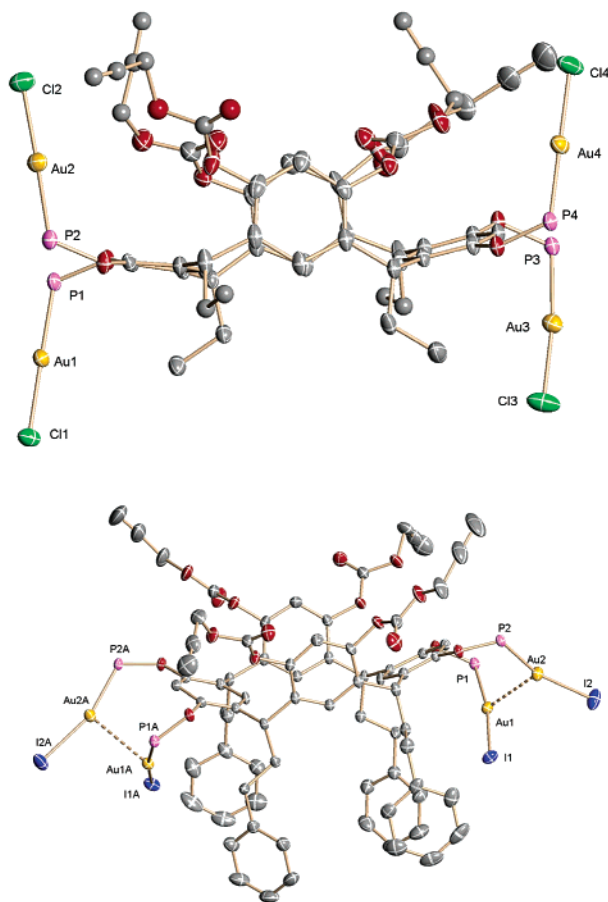
1–5 to give the chloride derivatives **6a–10a**, followed by halide exchange to give the corresponding bromide (**6b–10b**) or iodide (**6c–10c**) derivatives.

The digold(I) complexes **11–15** (Scheme 2) could be prepared by reaction of equimolar amounts of the appropriate tetraphosphinite ligand **1–5** with the corresponding tetragold(I) complex **6–10** or, less conveniently, by direct reaction of the ligand **1–5** with 2 molar equiv of $[\text{AuCl}(\text{SMe}_2)]$.

Structures of the Complexes in the Solid State. The structures of two (tetrakis(propargyl carbonato)tetraphosphinitoresorcinarene)tetragold(I) complexes, **6a,c**, were determined (**6c** was crystallized as both the tetrahydrofuran and dichloromethane solvates, which have similar structures with crystallographic 2-fold symmetry). The structures of **6a** and **6c**·THF are shown in Figure 1a,b, with selected bond distances and angles in Table 1. No gold–gold contacts were observed in the solid-state structure of **6a** (closest intramolecular $\text{Au}\cdots\text{Au} = 6.32 \text{ \AA}$ and intermolecular $\text{Au}\cdots\text{Au} = 5.21 \text{ \AA}$), and the roughly linear P–Au–Cl units are clearly directed away from each other (Figure 1a). However, in **6c**, the P–Au–I units are arranged so as to give a short $\text{Au}\cdots\text{Au}$ contact. The distance $\text{Au}(1)\cdots\text{Au}(2) = 3.1620(4) \text{ \AA}$ in **6c**·THF and $3.005(2) \text{ \AA}$ in **6c**· CH_2Cl_2 , indicating a strong aurophilic attraction in each case.^{1–3,5} The presence of the aurophilic attraction in **6c**·THF is accompanied by a distortion of the P–Au–I units away from linearity (most distorted is $\text{P}(2)\text{Au}(2)\text{I}(2) = 162.52(4)^\circ$), and an analysis of the reasons for this was made. The approach was to generate dummy iodide atoms in idealized positions for linear P–Au–I groups. In such a structure the distance $\text{I}\cdots\text{I} = 3.48 \text{ \AA}$, which is considerably less than either the van der Waals distance

Table 1. Selected Bond Lengths and Angles for Complexes **6a**, **6c**·THF, **6c**·CH₂Cl₂, **7c**, and **8a,b**

	6a	6c ·THF	6c ·CH ₂ Cl ₂	7c	8a	8b
Au1–P1	2.217(2)	2.251(2)	2.211(6)	2.241(2)	2.215(1)	2.222(2)
Au2–P2	2.209(2)	2.245(2)	2.212(6)	2.243(2)	2.215(1)	2.225(2)
Au3–P3	2.203(2)			2.243(2)		
Au4–P4	2.205(2)			2.243(2)		
Au1–X1	2.285(2)	2.5633(5)	2.540(2)	2.5643(6)	2.269(2)	2.368(1)
Au2–X2	2.287(2)	2.5777(6)	2.545(2)	2.5613(6)	2.275(2)	2.348(2)
Au3–X3	2.270(2)			2.5703(8)		
Au4–X4	2.265(2)			2.5582(5)		
P1–Au1–X1	178.73(7)	169.56(4)	167.2(1)	166.04(5)	174.52(7)	173.64(7)
P2–Au2–X2	177.20(7)	162.52(4)	168.1(2)	170.36(4)	174.85(6)	172.64(8)
P3–Au3–X3	173.28(9)			172.85(5)		
P4–Au4–X4	178.49(9)			173.52(4)		

**Figure 1.** Views of the structures of (a) complex **6a**, showing a side view, with phenyl rings of the diphenylphosphinite and phenethyl groups omitted for clarity, and (b) complex **6c**·THF, with phenyl groups of the diphenylphosphinite units and THF molecules omitted for clarity (Au(1)··Au(2) = 3.1620(4) Å).

of I··I = 3.96 Å or the observed distance I··I = 4.48 Å.¹¹ There are other short nonbonded contacts that are relieved by the distortion of the P–Au–I groups from linearity, and a summary of these, and of all the close contacts observed in such idealized linear structures, is given in Table 2. It is clear that in **6c** the distortion of the P–Au–I units arises to minimize steric congestion while allowing the aurophilic attraction to be present.

The resorcinarene skeleton adopts a boat conformation in both **6a,c**, with the acylated rings in the upright position and the phosphinite-derivatized rings in the flattened position.

In **6a**, the angles between the planes of opposite acylated rings and phosphinite-derivatized rings (fold angles) are 1 and 157°, respectively. The resorcinarene skeleton of **6a** is somewhat twisted, as can be seen by the dihedral angles between opposing resorcinol rings of 9 and 12° for the upright and flattened rings, respectively. The corresponding fold angles for **6c**·THF and **6c**·CH₂Cl₂ are 24 and 44° for the acylated rings and 137 and 128° for the flattened rings, and the large differences from the values for **6a** are rationalized in terms of the different conformation of the OPAuX groups needed to allow the Au··Au interaction in **6c** (Figure 1). The twist distortions, as measured by the dihedral angles between opposite rings, are slightly greater in **6c** than for **6a**, at 12° for the upright and 18° for the flattened rings in the THF solvate. The conformational parameters for the resorcinarene skeletons of all complexes studied are listed in Table 3.

The structure of the (tetrakis(benzyl carbonato)tetraphosphinitoresorcinarene)tetragold(I) complex **7c** is shown in Figure 2, with selected bond parameters in Table 1. The resorcinarene is again in the boat conformation, but remarkably, the acylated rings are now in the flattened position and near planar (fold angle = 175°), while the phosphinite-derivatized rings are upright and tilted slightly inward (fold angle = –8°, the negative sign indicating an inward tilt). This is the reverse of the boat conformations found in complexes **6a,c** (Figure 1 and Table 3) and also of the parent ligand **2**.¹⁰ This structural characterization of both C_{2v} boat conformations of the same parent resorcinarene is unprecedented.¹² There is very little twisting of the resorcinarene skeleton in **7c**, as measured by the dihedral angles between opposite rings (2° for the upright rings, 1° for the flattened rings).

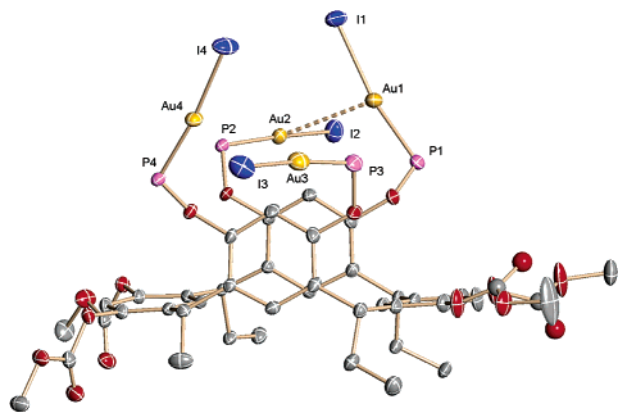
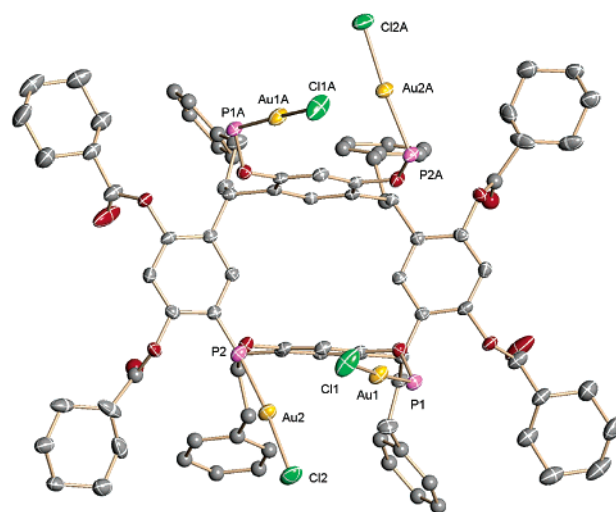
There is one weak aurophilic attraction in **7c** with Au(1)··Au(2) = 3.2483(4) Å, while the second close contact, Au(3)··Au(4) = 3.64 Å, is roughly equal to the van der Waals distance of 3.60 Å.² Nevertheless, these P–Au–I units are distorted from linearity, with PAuI = 172.85(5) and

(11) Bondi, A. *J. Phys. Chem.* **1964**, *68*, 441.(12) (a) Wieser, C.; Dieleman, C. B.; Matt, D. *Coord. Chem. Rev.* **1997**, *165*, 93. (b) Gutsche, C. D. *Calixarenes Revisited*; Monographs in Supramolecular Chemistry; The Royal Society of Chemistry: Cambridge, U.K., 1998. (c) Timmerman, P.; Verboom, W.; Reinhoudt, D. N. *Tetrahedron* **1996**, *52*, 2663. (d) Bohmer, V. *Angew. Chem., Int. Ed. Engl.* **1995**, *35*, 713. (e) Shivanyuk, A.; Paulus, E. F.; Bohmer, V.; Vogt, W. *J. Org. Chem.* **1998**, *63*, 6448. (f) Shivanyuk, A.; Paulus, E. F.; Bohmer, V. *Angew. Chem., Int. Ed.* **1999**, *38*, 2906. (g) Shivanyuk, A.; Paulus, E. F.; Rissanen, K.; Kolehmainen, E.; Bohmer, V. *Chem.—Eur. J.* **2001**, *7*, 1944. (h) Shivanyuk, A. *Chem. Commun.* **2001**, 1472.

Table 2. Close Contacts Observed for Idealized Linear P–Au–X Groups

complex	contact	D_i (Å)	R^{vdW} (Å) ^b	D_t (Å)	P–Au–X ^d	angle (deg)	complex	contact	D_i (Å)	R^{vdW} (Å) ^b	D_t (Å)	P–Au–X ^d	angle (deg)
6a	Cl3··H	2.77	2.95	2.93	P3–Au3–Cl3	173.28(9)	7c	I4··Au3	3.64	3.78	3.88		
6c·THF	I1··Au2	3.44	3.78	3.58				I4··H	3.01	3.18	3.22	P4–Au4–I4	173.52(4)
	I1··I2	3.48	3.96	4.48	P1–Au1–I1	169.56(4)	8a	Cl2··H	2.74	2.95	2.88	P2–Au2–Cl2	174.85(6)
	I2··Au1	3.51	3.78	3.58	P2–Au2–I2	162.52(4)	8b	Br2··H	2.76	3.05	2.95	P2–Au2–Br2	173.64(7)
6c·CH₂Cl₂	I1··Au2	3.37	3.78	3.64			8c	I1··I2	3.85	3.96	4.40		
	I1··I2	3.73	3.96	4.58	P1–Au1–I1			I1··H	2.94	3.18	3.20	P1–Au1–I1	171.33(7)
	I2··Au1	3.32	3.78	3.74	P2–Au2–I2		10a	I2··Au1	3.60	3.78	3.87	P2–Au2–I2	172.72(7)
7c	I1··Au2	3.35	3.78	3.87				Cl1··H	2.62	2.95	2.84	P1–Au1–Cl1	174.44(10)
	I1··I2	3.75	3.96	4.52	P1–Au1–I1	166.04(5)		Cl3··H	2.48	2.95	2.81	P3–Au3–Cl3	171.59(6)
	I2··Au1	3.48	3.78	3.85	P2–Au2–I2	170.36(4)	10c	I2··H	3.02	3.18	3.28		
	I3··Au4	3.94	3.78	4.20				I2··H	3.09	3.18	3.34	P2–Au2–I2	174.18(4)
	I3··H	2.85	3.18	3.12				I4··H	3.13	3.18	3.41		
	I3··I4	3.87	3.96	4.26	P3–Au3–I3	172.85(5)		I4··H	2.67	3.18	3.00	P4–Au4–I4	171.66(4)

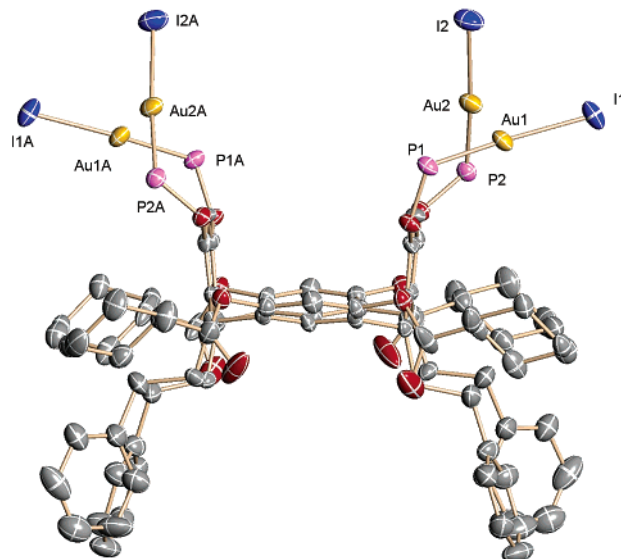
^a D_i = distance for idealized linear PAuX. ^b D_t = observed distance for bent PAuX. ^c R^{vdW} = sum of the van der Waals radii. ^d P–Au–X = group affected by contacts.

**Figure 2.** View of the structure of complex **7c**, with phenyl rings of the diphenylphosphinite and phenethyl groups omitted for clarity (Au(1)··Au(2) = 3.2483(4) Å).**Table 3.** Conformational Parameters for the Resorcinarene Skeletons of the Complexes

complex	fold angle ArOP (deg)	fold angle ArOC (deg)	twist angle ArOP (deg)	twist angle ArOC (deg)	Au··Au (Å)
6a	157	1	12	9	6.32
6c·THF	137	24	18	12	3.16
6c·CH₂Cl₂	128	44	20	12	3.00
7c	–8	175	2	1	3.25, 3.64
8a	12	151	5	5	3.75
8b	11	152	4	4	3.65
8c	11	154	4	4	3.62
9a	162	13	2	3	6.41, 6.43
10a	151	7	4	2	6.46, 6.62
10b	158	15	21	20	4.01
10c	156	7	4	4	6.45, 6.55

173.52(4)°, in the manner expected if there were an auriphilic interaction (Table 2),^{1–5,13} and so it is likely that a very weak auriphilic interaction is present.^{1–3,5,6,13} A partial structure determination for **7a** was completed and confirmed the same conformation is present as for **7c**, but poor crystal quality prevented full refinement.

The structures of the (tetrakis(cyclohexylcarboxylato)-tetraphosphinitoresorcinarene)tetrargold(I) complexes **8a–c** are similar and are illustrated for **8a,c** in Figure 3. Selected data are listed in Tables 1–4. In all three structures, the

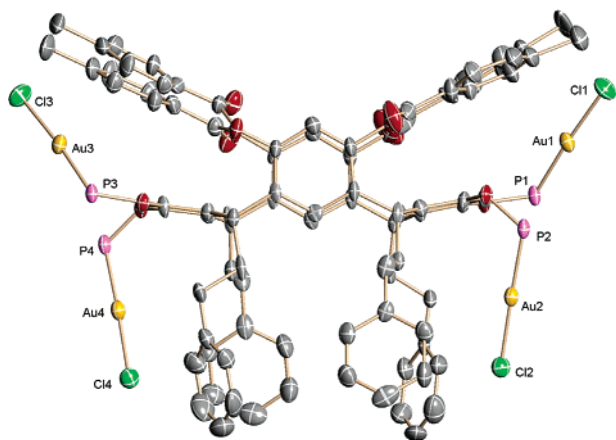
**Figure 3.** View of the structures of (a) complex **8a** and (b) complex **8c**. Phenyl rings of the diphenylphosphinite groups are omitted for clarity.

acylated arene rings are flattened and the phosphinite-derivatized arene groups are upright, with parameters given in Table 3. The intramolecular Au··Au distances (**8a**, 3.75; **8b**, 3.65; **8c**, 3.62 Å) follow the sequence AuCl > AuBr > AuI, as expected if these represent weak auriphilic attrac-

(13) Papatthanasious, P.; Salem, G.; Waring, P.; Willis, A. C. *J. Chem. Soc., Dalton Trans.* **1997**, 3435.

Table 4. Selected Bond Distances and Angles for Complexes **8c**, **9a**, and **10a–c**

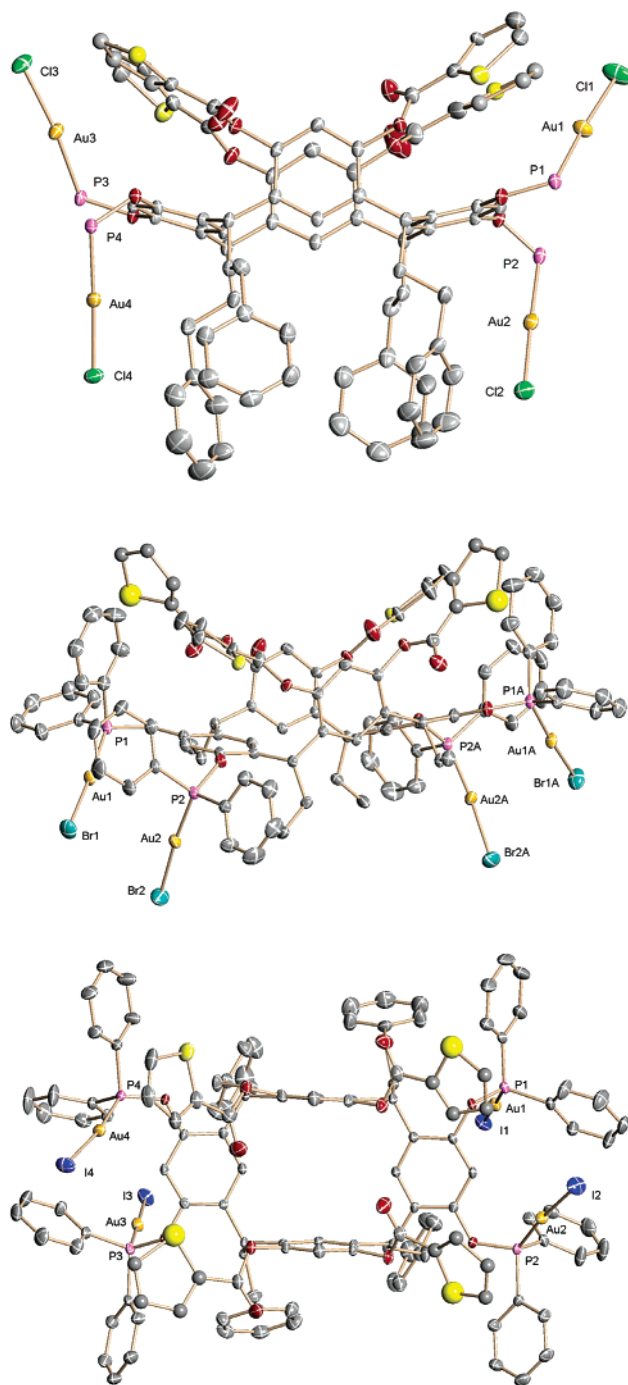
	8c	9a	10a	10b	10c
Au1–P1	2.236(2)	2.217(4)	2.215(2)	2.218(2)	2.240(2)
Au2–P2	2.240(3)	2.217(4)	2.214(2)	2.219(2)	2.238(2)
Au3–P3		2.213(4)	2.219(2)		2.234(2)
Au4–P4		2.223(4)	2.216(2)		2.235(2)
Au1–X1	2.5522(9)	2.274(4)	2.279(2)	2.3899(10)	2.5438(6)
Au1–X2	2.5491(7)	2.280(4)	2.269(2)	2.3636(10)	2.5466(6)
Au3–X3		2.270(4)	2.287(2)		2.5456(5)
Au4–X4		2.268(4)	2.274(2)		2.5496(5)
P1–Au1–X1	171.33(7)	175.9(2)	174.44(10)	176.00(6)	179.07(5)
P2–Au2–X2	172.72(7)	178.0(1)	178.13(6)	174.55(5)	174.18(4)
P3–Au3–X3		174.7(2)	171.59(6)		179.41(4)
P4–Au4–X4		177.4(1)	178.00(6)		171.66(4)

**Figure 4.** View of the structure of complex **9a**, with phenyl rings of the diphenylphosphinite groups omitted for clarity.

tions, but all are longer than the van der Waals distance of 3.60 Å.^{6,7} The mean P–Au–X bond angle follows the sequence **8a**, 174.7, **8b**, 172.6, and **8c**, 172.0°, and the somewhat greater distortion for the heavier halide derivatives is consistent with the trend in Au··Au distances, with shorter distances giving greater bond angle distortions (Table 1). There were few close contacts that could explain the observed distortions from linearity (Table 3).

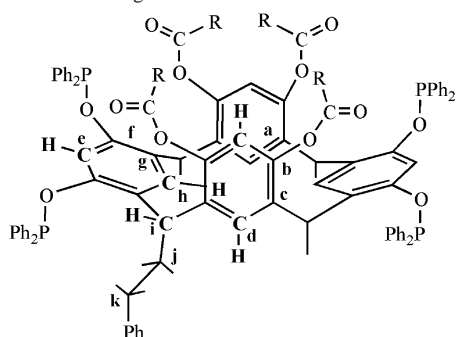
The structure of the (tetrakis(4-methylbenzoato)tetrphosphinitoresorcinarene)tetrargold(I) complex **9a** is shown in Figure 4, with structural parameters in Tables 2–4. The acylated arene rings are upright, and the phosphinite-derivatized rings are in the flattened position (Table 3). The tolyl groups are arranged in a roughly conical fashion over the top of the resorcinarene skeleton, with the faces perpendicular to the upright rings, giving an extended chalicelike appearance to the skeleton. The closest intramolecular and intermolecular Au··Au distances in **9a** are 6.43 and 7.38 Å, respectively, clearly showing the absence of aurophilic attractions, and the orientation of the P–Au–Cl units is similar to that in complex **6a**.

The structures of the (tetrakis(2-thiophenylcarboxylato)tetrphosphinitoresorcinarene)tetrargold(I) complexes **10a–c** are shown in Figure 5, with structural parameters in Tables 2–4. In each case, the acylated arene rings are in the upright position, with the thiophene substituents essentially perpendicular to the rings to give an extended chalicelike appearance to the resorcinarene skeleton, and the phosphinite-

**Figure 5.** Structure of (a) complex **10a**, (b) complex **10b**, and (c) complex **10c**. Phenyl rings of the diphenylphosphine or phenethyl groups are omitted for clarity in some cases.

derivatized rings are in the flattened position (Table 3). In complexes **10a,c**, the P–Au–X units are directed away from each other and so the Au··Au distances are well outside the range for aurophilic attractions (Table 3), but in complex **10b**, they are directed toward each other. Nevertheless, the distance Au··Au = 4.01 Å is not consistent with an aurophilic bond. In this conformation of complex **10b**, with all P–Au–Br units directed toward the lower rim of the resorcinarene skeleton, there is steric congestion that causes distortions of the resorcinarene skeleton, as discussed earlier for complex **6c** (Table 3). It is noteworthy that the thiophene

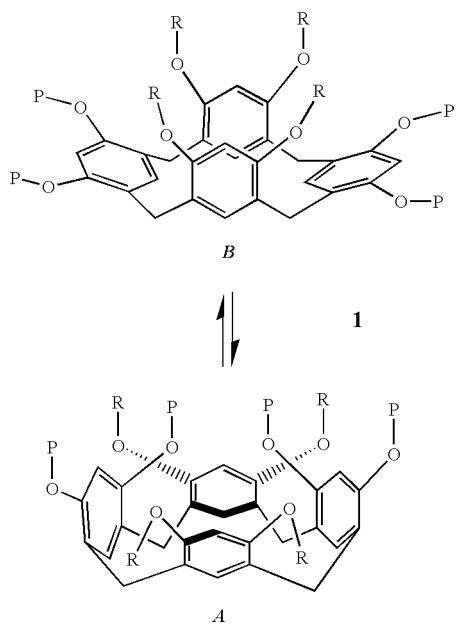
Chart 2. NMR Labeling



units do not complex to gold in any of the complexes **10a–c**.

Conformations of Complexes 6–10 in Solution As Determined by NMR. From the solid-state structures described above, it is clear that the complexes can exist in either boat conformation, with the preferred conformer depending on the ester derivative (Table 3). It is interesting then to determine if these conformations are retained in solution and if the conformers can interconvert easily. This was accomplished by using variable-temperature NMR methods (Chart 2 shows the NMR-labeling scheme used).¹⁰ The room-temperature ¹H NMR spectra of most of the tetragold(I) complexes were broad and poorly resolved as a result of fluxionality, involving interconversion between boat conformers **A** and **B** (eq 1, P = PPh₂AuX, R = acyl; **A** and **B** have phosphinite-derivatized rings upright and flat, respectively), but this exchange could be frozen out at low temperature. The variable-temperature ¹H and ³¹P NMR spectra of complex **7c** are shown in Figures 6 and 7.

At 253 K, the ¹H NMR spectrum of **7c** in the region of the methine protons (CHⁱ, Chart 2) and PhCH₂O protons resolves and shows the presence of both conformers **A** and **B** (eq 1), in approximately a 4:1 ratio (Figure 6). Each



conformer shows one resonance for the bridging methine protons and one AB quartet for the diastereotopic methylene

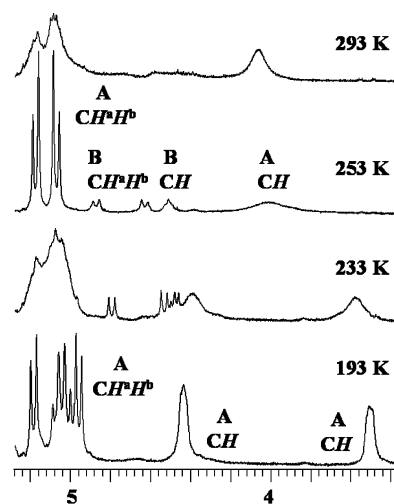


Figure 6. Variable-temperature ¹H NMR spectra of complex **7c**.

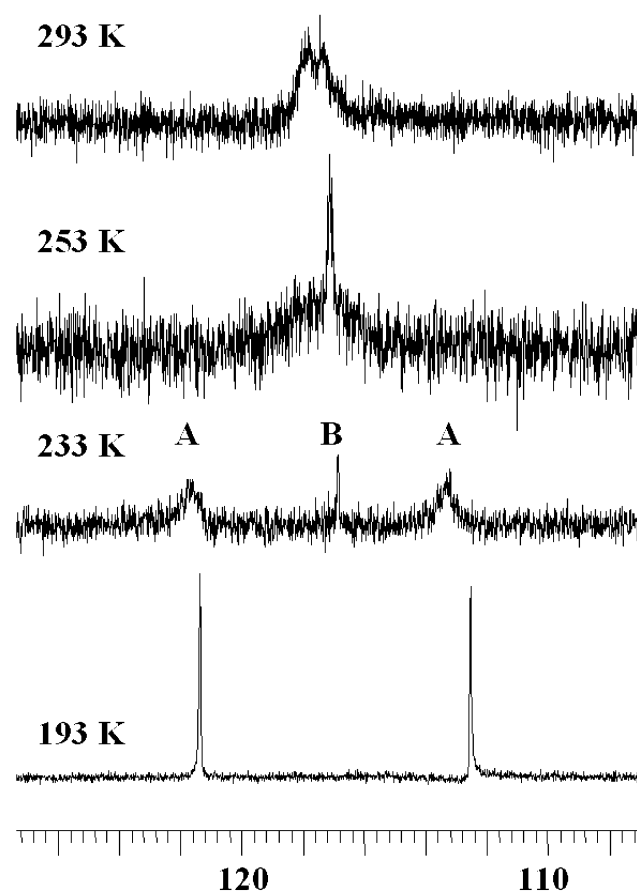


Figure 7. Variable-temperature ³¹P NMR spectra of complex **7c**.

protons of the OC(O)OCH₂Ph groups, as expected for a complex with C_{2v} symmetry. The room-temperature ³¹P NMR spectrum of **7c** (Figure 7) contains two broad resonances, and at 253 K, the spectrum contains a sharp singlet (minor component) superimposed on a broad peak (major component), corresponding to the two conformers. The conformers can be assigned from the arene resonances CH^b and CH^d (Chart 2), since CH^b in the flattened ring is more shielded, and these resonances are in turn assigned from the ¹H-, ¹³C-, gHSQC-, and gHMBC-correlated NMR spectra (Tables 5

Table 5. ^1H NMR Chemical Shifts^a (ppm) of Skeletal Ring Hydrogen Atoms

complex	a	d	e	h	complex	a	d	e	h
7a, A	7.29	6.04	7.37	7.32	9a, B	6.59	7.64	7.22	6.80
7a, B	6.71	7.55	6.89	6.39	10a, B	6.90	7.69	6.83	6.44
7c, A	7.28	6.07	7.53	7.36	11b	6.96	6.51	6.68	7.63
7c, B	6.61	7.51	7.03	6.40	12b	7.02	6.47	6.63	7.60
8a, A	6.98	6.31	7.61	7.51	13b	6.56	6.58	6.76	7.73
8a, B	6.63	7.56	7.00	6.25	13c	6.76	6.36	6.69	7.74

^a Not all resonances were directly observed in the ^1H NMR spectra; thus, some chemical shifts were obtained from the 2D NMR data.

Table 6. ^{13}C NMR Chemical Shifts^a (ppm) of Skeletal Ring Carbon Atoms

complex	a	b	c	d	e ^b	f	g	h
7a, A	114.26	146.00	133.92	126.42	112.18	n.o. ^c	n.o.	127.30
7a, B	116.95	147.94	131.67	124.86	107.84	149.40	132.24	n.o.
7c, A	114.33	146.09	134.04	126.31	111.63	n.o.	n.o.	127.40
7c, B	116.94	147.99	131.59	n.o.	108.39	149.89	132.05	n.o.
8a, A	117.01	146.46	130.62	n.o.	111.83	150.63	129.48	n.o.
8a, B	118.13	149.03	129.83	n.o.	108.67	149.70	133.15	n.o.
9a, B	119.37	149.66	131.93	121.71	108.78	149.72	134.08	129.43
10a, B	118.57	148.62	131.44	126.41	108.54	149.63	133.01	128.51
11b	114.94	146.46	133.89	126.36	114.51	151.95	128.45	129.21
12b	115.24	146.67	133.68	126.17	114.03	151.89	128.45	129.12
13b	117.70	146.73	134.01	126.28	114.56	152.06	128.65	129.65
13c	117.23	146.79	134.25	126.28	110.47	151.57	127.06	129.22

^a Not all resonances were directly observed in the ^{13}C NMR spectra; thus, some chemical shifts were obtained from the 2D NMR data. ^b In each case this resonance appears as a multiplet. ^c The resonance for this carbon atom was not observed.

Table 7. ^{31}P NMR Chemical Shifts (ppm) of Complexes **6a–10c**

complex	T (K)	A	B	T (K)	A	B
6a	253	115.12	110.90	213	113.30, 116.25	110.28
6b	253	116.10	112.98	193	113.13, 117.89	112.98
6c	253	117.89	116.99	213	113.91, 121.86	116.85
7a	273	114.44	111.48	213	112.41, 115.80	110.76
7b	253	115.67	113.24	213	112.41, 117.60	112.80
7c	253	118.00	117.01	223	113.18, 121.57	116.76
8a	293	112.17	111.97	213	110.21, 113.45	112.10
8b	293	113.87	113.64	213	111.47, 115.28	113.51
8c	293	116.69	116.69	213	112.14, 119.87	116.09
9a	293	113.44	111.57	193	110.15, 114.90	111.52
9b	293	113.95	113.32			
9c	293	117.04	117.04	193	111.09, 120.63	117.31
10a	293	112.98	111.10	193		109.5 (br)
10b	293	113.98	112.78	193		110.4 (br)
10c	253	116.39	116.39	193	112.26, 120.91	115.9 (br)

and **6**).¹⁰ Thus, for complex **7c**, the ratio of conformers **A**:**B** = 4:1 at 253 K, and the major conformer is the one which was present in the solid-state structure (Figure 2). The ^{31}P NMR data for all complexes are summarized in Table 7, and equilibrium constants for eq 1, and the derived thermodynamic data, are in Table 8 for those complexes for which it was possible to measure the equilibrium constants over a range of temperatures. In all cases, the enthalpy term favored conformer **A** but the entropy term favored conformer **B**, and so the equilibrium constants were temperature dependent and the favored conformer in solution depended on whether the enthalpy or entropy term was dominant. The dominant conformer in solution was the one that crystallized in most cases, the only exception being complex **6c**. In this case, conformer **A** was dominant in solution but conformer **B** was present in the solid state (Figure 1). The temperature dependence of the equilibrium constant for complex **7c** is

clearly shown in Figures 6 and 7; the conformer **B** was not present in detectable quantity at 193 K.

The interconversion between equivalent C_{2v} boat conformations of resorcinarenes is well-known,¹² but this appears to be the first case in which both possible C_{2v} conformers of an unsymmetrical resorcinarene are shown to be present in solution and taking part in conformational switching.¹⁴ The variable-temperature NMR spectra of the parent ligand **2** did not provide evidence for fluxionality, but it is probable that **2** is also fluxional, with a much lower energy barrier compared to **7c**, so that the interconversion between conformers cannot be frozen out. Thus, the increase in this energy barrier as a result of the addition of gold halide units appears to be important in allowing the first direct observation of boat–boat transitions in resorcinarenes containing different substituents on opposing resorcinol arene rings.

At 193 K, the ^1H and ^{31}P NMR spectra of complex **7c** split further and show a pattern consistent with a C_2 symmetrical conformer **A** of **7c** (Figures 6 and 7). Two resonances are observed for the bridging methine protons, two AB quartets for the methylene protons of the OC(O)-OCH₂Ph groups in the ^1H NMR (Figure 6), and two sharp singlets in the ^{31}P NMR (Figure 7). The interconversion between the C_2 conformers by way of a C_{2v} intermediate is depicted in Scheme 3. The equilibration between C_2 conformers of **A** leads to effective C_{2v} symmetry in the spectra at 253 K, while the less rigid conformer **B** maintains effective C_{2v} symmetry to 213 K, the lowest temperature that it was detected. The broad spectra at room-temperature arise from the onset of exchange between conformers **A** and **B** (eq 1). The activation energies for interconversion between the C_2 conformers **A** are summarized in Table 9. Conformer **A** is more rigid than **B** (Table 8), probably because the phenyl groups of the diphenylphosphinite substituents are more tightly packed, and so it is natural that the C_2 – C_2 fluxionality has a higher barrier for **A** than for **B**.

The NMR spectra of complex **6a** illustrate the temperature dependence of the equilibrium constant $K = [\text{A}]/[\text{B}]$. There is a preference for conformation **B** at room temperature [$K_{\text{eq}} = 0.3(1)$ at 293 K], but at 233 K, **A** and **B** are present in approximately equal proportions and, finally, at 193 K, **A** is favored (K_{eq} ca. 2.4). In this case, conformer **B** is still present in significant quantities at 193 K, but the ^1H and ^{31}P NMR spectra do not split to give the C_2 pattern seen for conformer **A**.

Characterization of the Digold Complexes **11–15**.

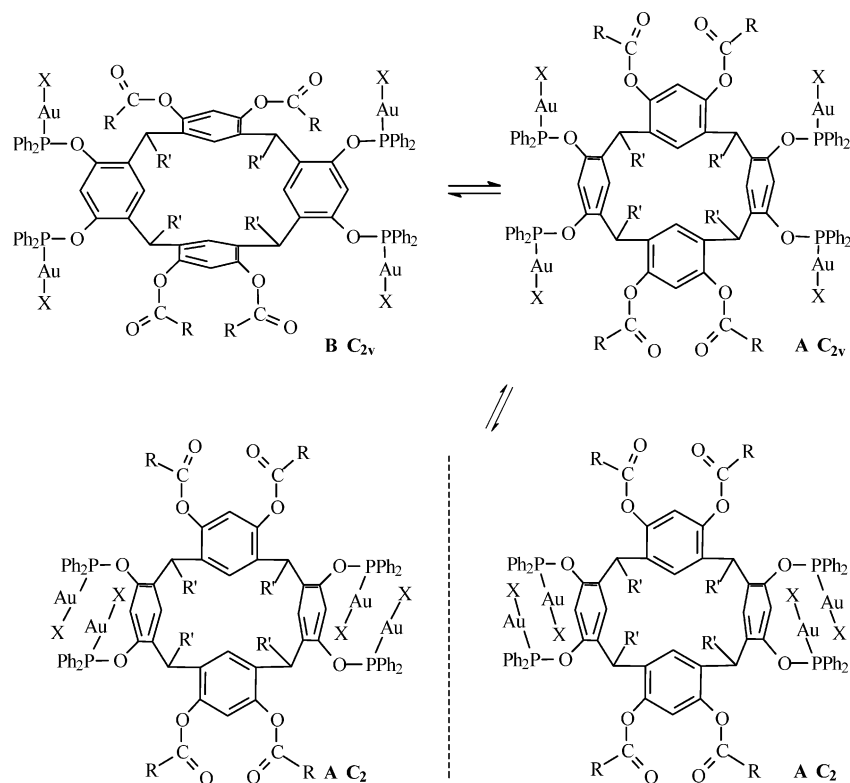
These complexes (Scheme 2) did not give crystals suitable for structure determination, and so they were characterized by their NMR spectra. The ^{31}P NMR spectra obtained on sequential addition of ligand **1** to a solution of complex **6a** in CD_2Cl_2 are shown in Figure 8. When less than 1 equiv of ligand was added, a mixture of the tetragold and digold

- (14) (a) Lukin, O.; Shivanyuk, A.; Pirozhenko, V.; Tsybal, I. F.; Kalchenko, V. I. *J. Org. Chem.* **1998**, *63*, 9510. (b) Shivanyuk, A.; Schmidt, C.; Bohmer, V.; Paulus, E. F.; Lukin, O.; Vogt, W. *J. Am. Chem. Soc.* **1998**, *120*, 4319. (c) Luostarinen, M.; Shivanyuk, A.; Rissanen, K. *Org. Lett.* **2001**, *3*, 4141. (d) Shivanyuk, A.; Far, A. R.; Rebek, J., Jr. *Org. Lett.* **2002**, *4*, 1555.

Table 8. Equilibrium and Thermodynamic Data for Complexes **6a–10c**

complex	$K_{\text{eq}},^a T$ (K)	K_{eq}, T (K)	K_{eq}, T (K)	K_{eq}, T (K)	ΔH (kJ)	ΔS (J K ⁻¹ mol ⁻¹)	ΔG (293 K)
6a	0.3(1), 293	0.4(1), 273	0.6(1), 253	0.9(1), 233	-9.6(5)	-42.2(4)	2.8
6b	0.6(1), 293	0.9(1), 273	2.3(3), 213		-8(1)	-32(1)	1.0
6c	2.0(3), 273	3.2(5), 253	6(1), 213		-8.5(3)	-24.7(3)	-1.2
7a	1.6(2), 293	3.0(5), 253	5(1), 233		-10.8(6)	-33.3(4)	-0.9
7c	4(1), 243	6(2), 233	8(3), 213		-12.0(6)	-39.1(3)	-1.2
9a	0.2(1), 293	0.5(1), 213	0.6(1), 193		-5.3(1)	-31.4(2)	3.8

^a $K_{\text{eq}} = [\text{A}]/[\text{B}]$. ^b $K_{\text{eq}}(253)$ **7b** = 3(1). ^c $K_{\text{eq}}(273)$ **8a** = 4(1). ^d $K_{\text{eq}}(213)$ **8b** = 7(2). ^e $K_{\text{eq}}(213)$ **8c** = 8(3). ^f $K_{\text{eq}}(253)$ **9b** = 0.3(1). ^g $K_{\text{eq}}(193)$ **9c** = 3(1). ^h $K_{\text{eq}}(293)$ **10a** = 16(4). ⁱ $K_{\text{eq}}(293)$ **10b** = 14(3). ^j $K_{\text{eq}}(193)$ **10c** = 13(3).

Scheme 3**Table 9.** Activation Energy for C₂-C₂ Interconversion of Conformer A

complex	ΔG^* (kJ mol ⁻¹)	coalescence T (K)	complex	ΔG^* (kJ mol ⁻¹)	coalescence T (K)
6a	46(1)	243	8a	41(1)	213
6b	46(1)	243	8b	41(1)	213
6c	46(1)	243	8c	41(1)	213
7a	46(1)	243	9a	45(1)	233
7b	46(1)	233	9c	44(1)	233
7c	46(1)	243	10c	44(1)	233

complexes **6a** and **11a** was present (Figure 8b), with the easy redistribution made possible by the lability of the gold(I) centers.^{1,3-5,7} When 1 equiv of ligand **1** was added, only the digold complex **11a** was present (Figure 8c) and addition of more ligand **1** resulted in the appearance of a resonance for the free ligand along with that for **11a** (Figure 8d). These data show that only the digold(I) and tetragold(I) complexes are formed in detectable quantity and also that **11a** appears to be formed as a single conformer.

The room-temperature ¹H NMR spectrum of complex **11a** is much sharper and well-resolved compared to **6a** and remains essentially unchanged at 193 K, indicating that **11a**

exists as a single conformer. Several coordination environments have been observed for gold halide complexes with phosphine ligands, including [AuXL₂], [AuXL₃], and [AuL₃]X.^{8,15-16} In general, only the complexes [AuXL₂] have a higher ³¹P NMR chemical shift than the parent complexes [AuXL],¹⁵ so complexes **11–15**, whose ³¹P NMR chemical shifts are listed in Table 10, are thought to have this type of coordination. The conformation of the resorcinarene skeleton in each of the complexes **11b**, **12b**, and **13b,c** was determined by NMR,¹⁰ and the compounds were shown to have the phosphinite-derivatized arene rings in the upright position (conformation A, eq 1). The structure proposed in Scheme 2 is consistent with all the data, but the structure is not uniquely defined.

- (15) (a) Bowmaker, G. A.; Dyason, J. C.; Healy, P. C.; Engelhart, L. M.; Pakawatchai, C.; White, A. H. *J. Chem. Soc., Dalton Trans.* **1987**, 1089. (b) Al-Baker, S.; Hill, W. E.; McAuliffe, C. A. *J. Chem. Soc., Dalton Trans.* **1986**, 1297. (c) Al-Baker, S.; Hill, W. E.; McAuliffe, C. A. *J. Chem. Soc., Dalton Trans.* **1985**, 2655. (d) Berners-Price, S. J.; Mazid, M. A.; Sadler, P. J. *J. Chem. Soc., Dalton Trans.* **1984**, 969. (e) Baenziger, N. C.; Dittmore, K. M.; Doyle, J. R. *Inorg. Chem.* **1974**, *13*, 805.
- (16) Bak, B.; Christensen, D.; Rastrup-Andersen, J.; Tannenbaum, E. *J. Chem. Phys.* **1956**, *25*, 892.

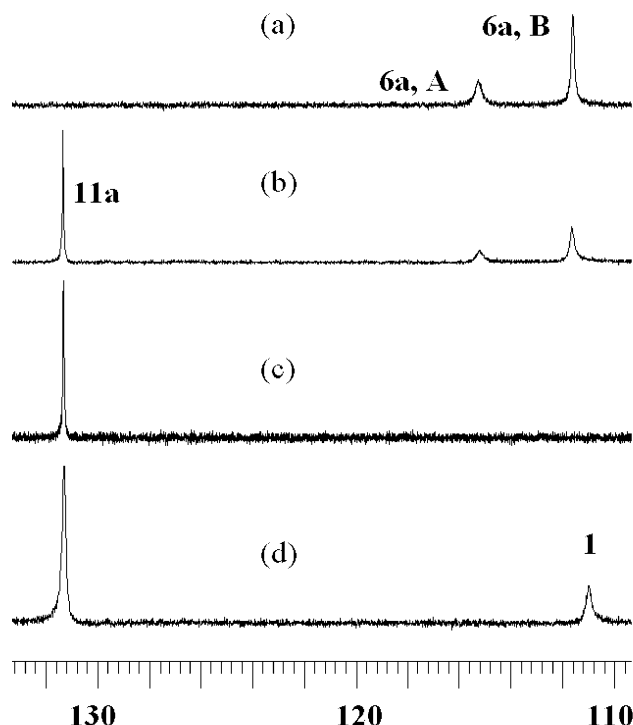


Figure 8. ^{31}P spectra showing sequential additions of ligand **1** to complex **6a** to form complex **11a**.

Table 10. Comparison of ^{31}P NMR of $[\text{Au}(\text{L})_2\text{X}]$ and $[\text{Au}(\text{L})\text{X}]$ at 293 K

	δ (ppm)	δ	$\Delta\delta^a$	δ	δ	$\Delta\delta^a$
11a	131.30	6a 111.58 115.23	+19.72 +16.07	13b 129.26	8b 113.64	+15.65 +15.39
11b	128.74	6b 113.42 116.11	+15.32 +12.63	13c 123.84	8c 116.69	+7.15
11c	123.24	6c 117.25	+5.99	14a 132.36	9a 111.57 113.44	+20.79 +18.92
12a	131.15	7a 111.77 114.65	+19.38 +16.50	14b 129.10	9b 113.32 113.95	+15.78 +15.15
12b	128.74	7b 113.64 115.70	+15.10 +13.04	14c 123.38	9c 117.04	+6.34
12c	123.11	7c 117.95	+5.16	15a 132.23	10a 111.10 112.98	+21.13 +19.25
13a	132.48	8a 111.97 112.49	+20.51 +19.99	15b 128.86	10b 112.78 113.98	+16.08 +14.88

$$^a \Delta\delta = \delta[\text{Au}(\text{L})_2\text{X}] - \delta[\text{Au}(\text{L})\text{X}].$$

Conclusions

The architecture of the tetraphosphinite resorcinarene compounds is such that formation of intramolecular Au \cdots Au interactions in the gold(I) derivatives is possible in either conformation **A** or **B**, as seen in the structures of the iodogold(I) complexes **7c** and **6c**, respectively, but it is accompanied by distortion of the resorcinarene skeleton in conformation **B**. There was little effect of the Au \cdots Au interactions on the skeleton of the resorcinarene in conformation **A**. No intermolecular Au \cdots Au interactions were observed in any of the structures obtained, probably because the bulk of the resorcinarene ligand prevents a close approach.

The presence of gold halide units increased the activation energy for boat–boat conformational exchange compared to the free ligands and so allowed these processes to be defined for the first time.¹³ In general, the preferred conformer in solution is the one that crystallizes, but one

exception was noted. In solution, the position of the equilibrium depends primarily on the nature of the ester group used, but there is also a dependence on the gold halide derivative. For complexes **6a–c**, for example, there was a clear shift in the equilibrium between the two conformers toward conformation **A** in the order of Cl < Br < I (Table 8). Clearly, tailoring of these resorcinarene complexes is possible to give complexes in a preferred conformation.

Experimental Section

All reactions were performed under a nitrogen atmosphere using standard Schlenk techniques. Solvents were freshly distilled, dried, and degassed prior to use. NMR spectra were recorded using a Varian Inova 400 NMR unless otherwise noted. Mass spectra were collected using an Applied Biosystems Mariner electrospray mass spectrometer. The complex $[\text{AuCl}(\text{SMe}_2)]$ and the tetraphosphinite resorcinarene ligands were prepared as previously reported.¹⁰ In the formulas below the resorcinarene skeleton ($\text{C}_6\text{H}_2\text{CH}\{\text{CH}_2\text{CH}_2\text{-Ph}\}_4$) is represented as resorcinarene. The proton and carbon resonances of the resorcinarene skeleton are identified according to the labeling scheme shown in Chart 2.

[Resorcinarene(OC(O)OCH₂C≡CH)₄(OPPh₂{AuCl})₄], 6a. A mixture of **1** (0.100 g, 0.051 mmol) and $[\text{AuCl}(\text{SMe}_2)]$ (0.060 g, 0.203 mmol) in CH_2Cl_2 (10 mL) in a darkened flask was stirred for 1 h. The solution was filtered through Celite, and a white solid was precipitated with *n*-pentane. The solid was collected, washed with diethyl ether (10 mL), and recrystallized from CHCl_3/n -hexane. Yield: 0.108 g, 73.4%. NMR [CD_2Cl_2 , 253 K; $\delta(^1\text{H})$]: (**A**, **B**) 2.06–2.66 [m, *Hⁱ*, *H^k*]; 6.00, 6.14, 6.72 [s, *Ar-H*]; 6.80–7.78 [m, *Ar-H*, *Ph*]; (**A**) 2.70 [br, 4H, $\text{OCH}_2\text{C}\equiv\text{CH}$]; 3.96 [br, 4H, *Hⁱ*]; 4.78 [m, 8H, $^2J_{\text{HH}} = 15$ Hz, $^4J_{\text{HH}} = 2$ Hz, $\text{OCH}_2\text{C}\equiv\text{CH}$]; (**B**) 2.56 [t, 4H, $^4J_{\text{HH}} = 2$ Hz, $\text{OCH}_2\text{C}\equiv\text{CH}$]; 4.47 [t, 4H, $^3J_{\text{HH}} = 7$ Hz, *Hⁱ*]; 4.64 [m, 8H, $^2J_{\text{HH}} = 15$ Hz, $^4J_{\text{HH}} = 2$ Hz, $\text{OCH}_2\text{C}\equiv\text{CH}$]. NMR [CD_2Cl_2 , 213 K; $\delta(^1\text{H})$]: (**A**, **B**) 1.18–2.73 [m, *Hⁱ*, *H^k*]; 5.97, 6.08, 6.58 [s, *Ar-H*]; 6.77–7.98 [m, *Ar-H*, *Ph*]; (**A**) 2.67 [br, 4H, $\text{OCH}_2\text{C}\equiv\text{CH}$]; 3.55, 4.33 [br, 4H, *Hⁱ*]; 4.75 [m, br, 8H, $\text{OCH}_2\text{C}\equiv\text{CH}$]; (**B**) 2.59 [t, 4H, $^4J_{\text{HH}} = 2$ Hz, $\text{OCH}_2\text{C}\equiv\text{CH}$]; 4.44 [t, 4H, $^3J_{\text{HH}} = 7$ Hz, *Hⁱ*]; 4.60 [m, 8H, $^2J_{\text{HH}} = 15$ Hz, $^4J_{\text{HH}} = 2$ Hz, $\text{OCH}_2\text{C}\equiv\text{CH}$]. Anal. Calcd for $\text{C}_{124}\text{H}_{100}\text{Au}_4\text{Cl}_4\text{O}_{16}\text{P}_4$: C, 51.36; H, 3.48. Found: C, 51.87; H, 3.57.

[Resorcinarene(OC(O)OCH₂C≡CH)₄(OPPh₂{AuBr})₄], 6b. A mixture of **1** (0.100 g, 0.051 mmol) and $[\text{AuCl}(\text{SMe}_2)]$ (0.060 g, 0.190 mmol) in CH_2Cl_2 (10 mL) in a darkened flask was stirred for 1 h. To this was added LiBr (0.018 g, 0.207 mmol), and the mixture was stirred for 16 h. The solution was filtered through Celite, and a white solid was precipitated with *n*-pentane. The solid was collected, washed with diethyl ether (10 mL), and recrystallized from CHCl_3/n -hexane. Yield: 0.088 g, 56.3%. NMR [CD_2Cl_2 , 253 K; $\delta(^1\text{H})$]: (**A**, **B**) 1.59–2.50 [m, *Hⁱ*, *H^k*]; 6.80–7.81 [m, *Ar-H*, *Ph*]; (**A**) 2.65 [br, 4H, $\text{OCH}_2\text{C}\equiv\text{CH}$]; 3.96 [br, 4H, *Hⁱ*]; 4.76 [m, 8H, $^2J_{\text{HH}} = 15$ Hz, $^4J_{\text{HH}} = 2$ Hz, $\text{OCH}_2\text{C}\equiv\text{CH}$]; 6.02 [s, 2H, *Ar-H*]; (**B**) 2.55 [s, br, $\text{OCH}_2\text{C}\equiv\text{CH}$]; 4.48 [t, 4H, $^3J_{\text{HH}} = 7$ Hz, *Hⁱ*]; 4.60 [m, 8H, $^2J_{\text{HH}} = 15$ Hz, $^4J_{\text{HH}} = 2$ Hz, $\text{OCH}_2\text{C}\equiv\text{CH}$]; 6.18 [s, 2H, *Ar-H*]. NMR [CD_2Cl_2 , 193 K; $\delta(^1\text{H})$]: (**A**, **B**) 1.15–2.60 [m, *Hⁱ*, *H^k*]; 6.61–8.02 [m, *Ar-H*, *Ph*]. (**A**) 2.73 [br, 4H, $\text{OCH}_2\text{C}\equiv\text{CH}$]; 3.49, 4.34 [br, 4H, *Hⁱ*]; 4.74 [m, br, 8H, $\text{OCH}_2\text{C}\equiv\text{CH}$]; 5.98 [s, 2H, *Ar-H*]; (**B**) 2.58 [br, 4H, $\text{OCH}_2\text{C}\equiv\text{CH}$]; 4.42 [br, 4H, *Hⁱ*]; 4.51 [m, br, 8H, $\text{OCH}_2\text{C}\equiv\text{CH}$]; 6.12 [s, 2H, *Ar-H*]. Anal. Calcd for $\text{C}_{124}\text{H}_{100}\text{Au}_4\text{Br}_4\text{O}_{16}\text{P}_4$: C, 48.39; H, 3.28. Found: C, 47.97; H, 3.34.

[Resorcinarene(OC(O)OCH₂C≡CH)₄(OPPh₂{AuI})₄], 6c. This was prepared similarly from **1** (0.100 g, 0.051 mmol), $[\text{AuCl}(\text{SMe}_2)]$

(0.060 g, 0.203 mmol), and NaI (0.031 g, 0.207 mmol) to produce a white solid. Yield: 0.090 g, 54.3%. NMR [CD₂Cl₂, 253 K; δ (¹H)]:

(A, B) 1.59–2.50 [m, Hⁱ, H^k]; 6.80–7.81 [m, Ar-H, Ph]; (A) 2.65 [br, 4H, OCH₂C≡CH]; 3.96 [br, 4H, CHCH₂CH₂Ph]; 4.76 [m, 8H, ²J_{HH} = 15 Hz, ⁴J_{HH} = 2 Hz, OCH₂C≡CH]; 6.02 [s, 2H, Ar-H]; (B) 2.55 [s, br, OCH₂C≡CH]; 4.48 [t, 4H, ³J_{HH} = 7 Hz, Hⁱ]; 4.60 [m, 8H, ²J_{HH} = 15 Hz, ⁴J_{HH} = 2 Hz, OCH₂C≡CH]; 6.18 [s, 2H, Ar-H]. NMR [CD₂Cl₂, 193 K; δ (¹H)]: (A) 1.16, 1.44, 1.68, 1.79, 1.91, 2.23, 2.56 [m, 16H, Hⁱ, H^k]; 2.60, 2.74 [s, br, 4H, OCH₂C≡CH]; 3.46, 4.38 [br, 4H, Hⁱ]; 4.69 [m, br, 4H, OCH₂C≡CH]; 4.73 [m, 4H, ²J_{HH} = 16 Hz, OCH₂C≡CH]; 6.10 [s, 2H, Ar-H]; 6.84–8.02 [m, 66H, Ar-H, Ph]. Anal. Calcd for C₁₂₄H₁₀₀-Au₄I₄O₁₆P₄: C, 45.61; H, 3.09. Found: C, 45.88; H, 3.32.

[Resorcinarene(OC(O)OCH₂Ph)₄(OPPh₂{AuCl})₄], **7a**. This was prepared similarly to **6a** from **2** (0.100 g, 0.046 mmol) and [AuCl(SMe₂)] (0.054 g, 0.184 mmol) to produce a white solid. Yield: 0.077 g, 53.6%. NMR [CD₂Cl₂, 600 MHz, 273 K; δ (¹H)]: (A, B) 1.62–2.52 [m, Hⁱ, H^k]; 6.90–7.84 [m, Ar-H, Ph]; (A) 4.03 [br, 4H, Hⁱ]; 5.17 [m, 8H, ²J_{HH} = 12 Hz, OCH₂Ph]; 6.04 [s, 2H, Hⁱ] (B) 4.57 [br, 4H, Hⁱ]; 4.85 [m, 8H, ²J_{HH} = 12 Hz, OCH₂Ph]; 6.39 [s, 2H, Hⁱ]; 6.71 [s, 2H, H^a]; 6.89 [s, 2H, H^a]. NMR: δ (¹³C) (A, B) 125.93–133.58 [Ar-C, Ph]; (A) 33.20 [C^k]; 35.55 [Cⁱ]; 36.38 [C^j]; 70.54 [OC(O)OCH₂Ph]; 112.18 [m, C^e]; 114.26 [C^a]; 126.42 [C^d]; 127.30 [C^b]; 133.92 [C^c]; 134.69 [ipso-C, OCH₂Ph]; 140.93 [ipso-C, CH₂CH₂Ph]; 146.00 [C^b]; 152.81 [OC(O)OCH₂Ph]; (B) 34.34 [C^k]; 36.07 [Cⁱ]; 37.44 [C^j]; 70.05 [OC(O)OCH₂Ph]; 107.84 [m, C^e]; 116.95 [C^a]; 124.86 [C^d]; 132.24 [C^c]; 141.11 [ipso-C, CH₂CH₂Ph]; 147.94 [C^b]; 149.40 [d, ²J_{PC} = 5 Hz, C^f]; 152.36 [OC(O)OCH₂Ph]. NMR [CD₂Cl₂, 400 MHz, 193 K; δ (¹H)]: (A) 1.42, 1.55, 1.90, 2.18, 2.42 [m, 16H, Hⁱ, H^k]; 3.57, 4.42 [br, 4H, Hⁱ]; 5.07, 5.10 [m, 8H, ²J_{HH} = 12 Hz, OCH₂Ph]; 5.59 [s, 2H, Ar-H]; 6.80–7.80 [m, 86H, Ar-H, Ph]. Anal. Calcd for **7a**·0.5CHCl₃, C_{140.5}H_{116.5}Au₄Cl_{5.5}O₁₆P₄: C, 53.27; H, 3.71. Found: C, 53.50; H, 3.80.

[Resorcinarene(OC(O)OCH₂Ph)₄(OPPh₂{AuBr})₄], **7b**. This was prepared similarly to **6b** from **2** (0.100 g, 0.046 mmol), [AuCl(SMe₂)] (0.054 g, 0.184 mmol), and LiBr (0.016 g, 0.184 mmol) to produce a white solid. Yield: 0.090 g, 59.7%. NMR [CD₂Cl₂, 253 K; δ (¹H)]: (A, B) 1.66–2.49 [m, Hⁱ, H^k]; 6.85–7.85 [m, Ar-H, Ph]; (A) 4.02 [br, 4H, Hⁱ]; 5.16 [m, 8H, ²J_{HH} = 12 Hz, OCH₂Ph]; 6.04 [s, 2H, Ar-H]; (B) 4.55 [br, 4H, Hⁱ]; 4.79 [m, 8H, ²J_{HH} = 12 Hz, OCH₂Ph]; 6.39, 6.63 [s, 4H, Ar-H]. NMR [CD₂Cl₂, 193 K; δ (¹H)]: (A) 1.44, 1.61, 1.90, 2.17, 2.43 [m, 16H, Hⁱ, H^k]; 3.54, 4.41 [br, 4H, Hⁱ]; 5.09 [m, 4H, OCH₂Ph]; 5.10 [m, 4H, ²J_{HH} = 12 Hz, OCH₂Ph]; 6.00 [s, 2H, Ar-H]; 6.85–7.90 [m, 86H, Ar-H, Ph]. Anal. Calcd for C₁₄₀H₁₁₆Au₄Br₄O₁₆P₄: C, 51.18; H, 3.56. Found: C, 51.33; H, 3.65.

[Resorcinarene(OC(O)OCH₂Ph)₄(OPPh₂{AuI})₄], **7c**. This was prepared similarly from **2** (0.100 g, 0.046 mmol), [AuCl(SMe₂)] (0.054 g, 0.184 mmol), and NaI (0.028 g, 0.184 mmol) to produce a white solid. Yield: 0.092 g, 57.8%. NMR [CD₂Cl₂, 600 MHz, 253 K; δ (¹H)]: (A, B) 1.76–2.39 [m, Hⁱ, H^k]; 7.00–7.90 [m, Ar-H, Ph]; (A) 4.03 [br, 4H, Hⁱ]; 5.15 [m, 8H, ²J_{HH} = 12 Hz, OCH₂Ph]; 6.07 [s, 2H, H^d]; (B) 4.52 [br, 4H, Hⁱ]; 4.77 [m, 8H, ²J_{HH} = 12 Hz, OCH₂Ph]; 6.40 [s, 2H, H^a]; 6.61 [s, 2H, H^a]; δ (¹³C) (A, B) 125.93–133.58 [Ar-C, Ph]; (A) 33.33 [C^k]; 35.87 [Cⁱ]; 36.35 [C^j]; 70.56 [OC(O)OCH₂Ph]; 111.63 [m, C^e]; 114.33 [C^a]; 126.31 [C^d]; 127.40 [C^b]; 134.04 [C^c]; 134.51 [ipso-C, OCH₂Ph]; 141.05 [ipso-C, CH₂CH₂Ph]; 146.09 [C^b]; 152.84 [OC(O)OCH₂Ph]; (B) 34.22 [C^k]; 36.03 [Cⁱ]; 37.66 [C^j]; 70.15 [OC(O)OCH₂Ph]; 108.39 [m, C^e]; 116.94 [C^a]; 131.59 [C^c]; 132.05 [C^b]; 147.99 [C^b]; 149.89 [C^f]; 152.46 [OC(O)OCH₂Ph]. NMR [CD₂Cl₂, 400 MHz, 193 K; δ (¹H)]: (A) 1.45, 1.63, 1.91, 2.18, 2.43 [m, 16H, Hⁱ, H^k]; 3.51, 4.45 [br,

4H, Hⁱ]; 5.06, 5.10 [m, 8H, ²J_{HH} = 12 Hz, OCH₂Ph]; 6.03 [s, 2H, Ar-H]; 6.80–7.90 [m, 86H, Ar-H, Ph]. Anal. Calcd for C₁₄₀H₁₁₆-Au₄I₄O₁₆P₄: C, 48.41; H, 3.37. Found: C, 47.97; H, 3.59.

[Resorcinarene(OC(O)C₆H₁₁)₄(OPPh₂{AuCl})₄], **8a**. This was prepared similarly to **6a** from **3** (0.100 g, 0.048 mmol) and [AuCl(SMe₂)] (0.057 g, 0.194 mmol) to produce a white solid. Yield: 0.105 g, 72.6%. NMR [CD₂Cl₂, 293 K; δ (¹H)]: (A, B) 1.20–2.57 [m, Hⁱ, H^k, C₆H₁₁]; 6.81–7.80 [m, Ar-H, Ph]; (A) 4.38 [m, 4H, Hⁱ]; 6.31 [s, 2H, H^d]; 6.98 [s, 2H, H^a]; (B) 4.36 [m, 4H, Hⁱ]; 6.25 [s, 2H, H^b]; 6.63 [s, 2H, H^a]. NMR [CD₂Cl₂, 293 K; δ (¹³C)]: (A, B) 25.64, 25.83, 26.10, 28.97, 29.13, 29.20, 29.29, 42.95, 43.25 [C₆H₁₁]; 125.78–133.96 [Ar-C, Ph]; (A) 34.36 [C^k]; 36.22 [Cⁱ]; 37.67 [C^j]; 111.83 [m, C^e]; 117.01 [C^a]; 129.48 [C^b]; 130.62 [C^c]; 141.26 [ipso-C, Ph]; 146.46 [C^b]; 150.63 [d, ²J_{PC} = 5 Hz, C^f]; 174.01 [C=O]; (B) 34.74, 36.47 [Cⁱ, C^k]; 37.96 [C^j]; 108.67 [m, C^e]; 118.13 [C^a]; 129.83 [C^c]; 133.15 [C^b]; 141.10 [ipso-C, Ph]; 149.03 [C^b]; 149.70 [d, ²J_{PC} = 5 Hz, C^f]; 173.58 [C=O]. NMR [CD₂Cl₂, 183 K; δ (¹H)]: (A) 1.00–2.52 [m, 60H, Hⁱ, H^k, C₆H₁₁]; 3.91, 4.36 [br, 4H, Hⁱ]; 6.18 [s, 2H, Ar-H]; 6.60–8.02 [m, 66H, Ar-H, Ph]. Anal. Calcd for C₁₃₆H₁₃₂Au₄Cl₄O₁₂P₄: C, 54.23; H, 4.42. Found: C, 53.85; H, 4.56.

[Resorcinarene(OC(O)C₆H₁₁)₄(OPPh₂{AuBr})₄], **8b**. This was prepared similarly to **6b** from **3** (0.100 g, 0.048 mmol), [AuCl(SMe₂)] (0.057 g, 0.194 mmol), and LiBr (0.017 g, 0.195 mmol) to produce a white solid. Yield: 0.080 g, 52.2%. NMR [CD₂Cl₂, 293 K; δ (¹H)]: (A, B) 1.10–2.60 [m, Hⁱ, H^k, C₆H₁₁]; 6.80–7.80 [m, Ar-H, Ph]; (A) 4.32 [m, 4H, Hⁱ]; 6.27 [s, 2H, Ar-H]; (B) 4.37 [m, 4H, Hⁱ]; 6.23, 6.59 [s, 4H, Ar-H]. NMR [CD₂Cl₂, 193 K; δ (¹H)]: (A) 1.00–2.50 [m, 60H, Hⁱ, H^k, C₆H₁₁]; 3.87, 4.30 [br, 4H, Hⁱ]; 6.16 [s, 2H, Ar-H]; 6.64–7.98 [m, 66H, Ar-H, Ph]. Anal. Calcd for C₁₃₆H₁₃₂Au₄Br₄O₁₂P₄: C, 51.21; H, 4.17. Found: C, 50.80; H, 4.31.

[Resorcinarene(OC(O)C₆H₁₁)₄(OPPh₂{AuI})₄], **8c**. This was prepared similarly from **3** (0.100 g, 0.048 mmol), [AuCl(SMe₂)] (0.057 g, 0.194 mmol), and NaI (0.029 g, 0.194 mmol) to produce a white solid. Yield: 0.076 g, 46.9%. NMR [CD₂Cl₂, 293 K; δ (¹H)]: (A, B) 1.08–2.58 [m, Hⁱ, H^k, C₆H₁₁]; 6.82–7.85 [m, Ar-H, Ph]; (A) 4.28 [m, 4H, Hⁱ]; 6.26 [s, 2H, Ar-H]; (B) 4.46 [m, 4H, Hⁱ]; 6.31, 6.62 [s, 4H, Ar-H]. NMR [CD₂Cl₂, 193 K; δ (¹H)]: (A) 0.82–2.58 [m, 60H, Hⁱ, H^k, C₆H₁₁]; 3.76, 4.31 [br, 4H, Hⁱ]; 6.13 [s, 2H, Ar-H]; 6.70–7.88 [m, 66H, Ar-H, Ph]. Anal. Calcd for **8c**·0.5CH₂Cl₂, C_{136.5}H₁₃₃Au₄Cl₄O₁₂P₄: C, 47.93; H, 3.92. Found: C, 47.85; H, 4.12.

[Resorcinarene(OC(O)C₆H₄CH₃)₄(OPPh₂{AuCl})₄], **9a**. This was prepared similarly to **6a** from **4** (0.100 g, 0.047 mmol) and [AuCl(SMe₂)] (0.056 g, 0.190 mmol) to produce a white solid. Yield: 0.110 g, 76.4%. NMR [CD₂Cl₂, 293 K; δ (¹H)]: (A, B) 2.20, 2.44, 2.64 [m, Hⁱ, H^k]; 6.92–7.84 [m, Ar-H, Ph, C₆H₄CH₃]; (A) 2.47 [s, 12H, C₆H₄CH₃]; 4.34 [m, 4H, Hⁱ]; 6.41, 6.57 [s, 4H, Ar-H]; (B) 2.57 [s, 12H, C₆H₄CH₃]; 4.53 [m, 4H, Hⁱ]; 6.52, 6.72, 6.83 [s, 6H, Ar-H]. NMR [toluene-*d*₈, 20 °C; δ (¹H)]: (B) 4.76 [t, 4H, ²J_{HH} = 8 Hz, Hⁱ]; 6.59 [s, 2H, H^a]; 6.80 [s, 2H, H^b]; 7.22 [s, 2H, H^c]; 7.64 [s, 2H, H^d]. NMR [toluene-*d*₈; δ (¹³C)]: (B) 22.08 [C₆H₄CH₃]; 35.25 [C^k]; 37.18 [Cⁱ]; 37.89 [C^j]; 108.78 [m, C^e]; 119.37 [C^a]; 125.71 [C^d]; 126.30–133.69 [Ar-C, Ph]; 129.43 [C^b]; 131.93 [C^c]; 141.13 [ipso-C, CHCH₂CH₂Ph]; 134.08 [d, ³J_{PC} = 5 Hz, C^f]; 145.42 [ipso-C, C₆H₄CH₃]; 149.66 [C^b]; 149.72 [d, ²J_{PC} = 5 Hz, C^f]; 164.22 [C=O]. NMR [CD₂Cl₂, 193 K; δ (¹H)]: (A, B) 1.82–2.70 [m, Hⁱ, H^k]; 6.69–7.80 [m, Ar-H, Ph, C₆H₄CH₃]; (A) 2.39, 2.43 [s, 12H, C₆H₄CH₃]; 3.93, 4.51 [m, 4H, Hⁱ]; 6.32 [s, 2H, Ar-H]; (B) 2.50 [s, 12H, C₆H₄CH₃]; 4.43 [m, 4H, Hⁱ]; 6.46, 6.48 [s, 4H, Ar-H]. Anal. Calcd for C₁₄₀H₁₁₆Au₄Cl₄O₁₂P₄: C, 55.24; H, 3.84. Found: C, 55.43; H, 3.97.

[Resorcinarene(OC(O)C₆H₄CH₃)₄(OPPh₂{AuBr})₄], 9b. This was prepared similarly to **6b** from **4** (0.100 g, 0.047 mmol), [AuCl(SMe₂)] (0.056 g, 0.190 mmol), and LiBr (0.017 g, 0.195 mmol) to produce a white solid. Yield: 0.094 g, 61.7%. NMR [CD₂Cl₂, 293 K; δ(¹H)]: (A, B) 2.21–2.72 [m, Hⁱ, H^k]; 6.73–7.86 [m, Ar-H, Ph, C₆H₄CH₃]; (A) 2.47 [s, 12H, C₆H₄CH₃]; 4.34 [m, 4H, H^j]; 6.42, 6.59 [s, 4H, Ar-H]; (B) 2.58 [s, 12H, C₆H₄CH₃]; 4.55 [m, 4H, H^j]; 6.55 [s, 2H, Ar-H]. Anal. Calcd for C₁₄₀H₁₁₆Au₄Br₄O₁₂P₄: C, 52.19; H, 3.63. Found: C, 52.55; H, 3.86.

[Resorcinarene(OC(O)C₆H₄CH₃)₄(OPPh₂{AuI})₄], 9c. This was prepared similarly from **4** (0.100 g, 0.047 mmol), [AuCl(SMe₂)] (0.056 g, 0.190 mmol) and NaI (0.029 g, 0.193 mmol) to produce a white solid. Yield: 0.093 g, 57.7%. NMR [CD₂Cl₂, 293 K; δ(¹H)]: (A, B) 2.05–2.60 [m, Hⁱ, H^k]; 6.74–7.96 [m, Ar-H, Ph, C₆H₄CH₃]; (A) 2.47 [s, 12H, C₆H₄CH₃]; 4.32 [m, 4H, H^j]; 6.45, 6.53 [s, 4H, Ar-H]; (B) 2.55 [s, 12H, C₆H₄CH₃]; 4.54 [m, 4H, H^j]; 6.58 [s, 2H, Ar-H]. NMR [CD₂Cl₂, 193 K; δ(¹H)]: (A, B) 1.54–2.52 [m, Hⁱ, H^k]; 6.56–7.86 [m, Ar-H, Ph, C₆H₄CH₃]; (A) 2.41, 2.43 [s, 12H, C₆H₄CH₃]; 3.83, 4.51 [m, 4H, H^j]; 6.34 [s, 2H, Ar-H]; (B) 2.46 [s, 12H, C₆H₄CH₃]; 4.40 [m, 4H, H^j]. Anal. Calcd for C₁₄₀H₁₁₆Au₄I₄O₁₂P₄: C, 49.31; H, 3.43. Found: C, 48.86; H, 3.58.

[Resorcinarene(OC(O)C₄H₃S)₄(OPPh₂{AuCl})₄], 10a. This was prepared similarly to **6a** from **5** (0.100 g, 0.048 mmol) and [AuCl(SMe₂)] (0.057 g, 0.194 mmol) to produce a white solid. Yield: 0.120 g, 83.0%. NMR [CD₂Cl₂, 293 K; δ(¹H)]: (A, B) 2.14–2.62 [m, Hⁱ, H^k]; 6.88–7.70 [m, Ar-H, Ph, C₄H₃S]; (A) 4.73 [m, 4H, H^j]; 6.38, 6.56 [s, 4H, Ar-H]; (B) 4.53 [m, 4H, H^j]; 6.44 [s, 2H, H^h]; 6.83 [s, 2H, H^e]; 7.79, 8.03 [m, 8H, C₄H₃S]. NMR [CD₂Cl₂, 293 K; δ(¹³C)]: (B) 35.05 [C^k]; 37.42 [C^j]; 37.78 [Cⁱ]; 108.54 [m, C^e]; 118.57 [C^a]; 126.17–136.06 [Ar-C, Ph, C₄H₃S]; 126.41 [C^d]; 128.51 [C^h]; 131.44 [C^c]; 133.01 [d, ³J_{PC} = 5 Hz, C^g]; 141.22 [ipso-C, Ph]; 148.62 [C^b]; 149.63 [d, ²J_{PC} = 5 Hz, C^g]; 160.04 [C=O]. Anal. Calcd for C₁₂₈H₁₀₀Au₄Cl₄O₁₂P₄S₄: C, 51.04; H, 3.35. Found: C, 50.82; H, 3.33.

[Resorcinarene(OC(O)C₄H₃S)₄(OPPh₂{AuBr})₄], 10b. This was prepared similarly to **6b** from **5** (0.100 g, 0.048 mmol), [AuCl(SMe₂)] (0.057 g, 0.194 mmol), and LiBr (0.017 g, 0.195 mmol) to produce a white solid. Yield: 0.090 g, 58.8%. NMR [CD₂Cl₂, 293 K; δ(¹H)]: (A, B) 2.13–2.65 [m, Hⁱ, H^k]; 6.87–7.71 [m, Ar-H, Ph, C₄H₃S]; (A) 4.79 [m, 4H, H^j]; 6.39 [s, 2H, Ar-H]; (B) 4.55 [m, 4H, H^j]; 6.47 [s, 2H, Ar-H]; 7.79, 8.02 [m, 8H, C₄H₃S]. Anal. Calcd for **10b**•0.5CH₂Cl₂, C_{128.5}H₁₀₁Au₄Br₄ClO₁₂P₄S₄: C, 47.75; H, 3.15. Found: C, 47.60; H, 3.05.

[Resorcinarene(OC(O)C₄H₃S)₄(OPPh₂{AuI})₄], 10c. This was prepared similarly from **5** (0.100 g, 0.048 mmol), [AuCl(SMe₂)] (0.057 g, 0.194 mmol), and NaI (0.029 g, 0.194 mmol) to produce a white solid. Yield: 0.094 g, 58.0%. NMR [CD₂Cl₂, 253 K; δ(¹H)]: (A, B) 2.10–2.63 [m, Hⁱ, H^k]; 6.90–7.71 [m, Ar-H, Ph, C₄H₃S]; (A) 4.72 [m, 4H, H^j]; 6.37 [s, 2H, Ar-H]; (B) 4.50 [m, 4H, H^j]; 6.51, 6.81 [s, 4H, Ar-H]; 7.78, 7.98 [m, 8H, C₄H₃S]. NMR [CD₂Cl₂, 193 K; δ(¹H)]: (A, B) 1.90–2.58 [m, Hⁱ, H^k]; 6.76–7.93 [m, Ar-H, Ph, C₄H₃S]; (B) 4.43 [m, 4H, H^j]; 6.57 [s, 2H, Ar-H]. Anal. Calcd for **10c**•0.5CHCl₃, C_{128.5}H_{100.5}Au₄Cl_{1.5}I₄O₁₂P₄S₄: C, 44.90; H, 2.95. Found: C, 44.87; H, 3.04.

[Resorcinarene(OC(O)OCH₂C≡CH)₄(OPPh₂{AuCl})₂], 11a. A mixture of **6a** (0.0520 g, 0.0179 mmol) and **1** (0.0353 g, 0.0179 mmol) in CH₂Cl₂ (5 mL) in a darkened flask was stirred for 15 min. The solution was filtered through Celite, and a white solid was precipitated with *n*-pentane. Yield: 0.047 g, 53.4%. NMR [CD₂Cl₂; δ(¹H)]: 2.00, 2.30 [m, 8H, H^j]; 2.42, 2.74 [m, 8H, H^k]; 2.70 [t, 4H, ⁴J_{HH} = 2 Hz, OCH₂C≡CH]; 4.56 [m, 4H, Hⁱ]; 4.69 [m, 8H, ⁴J_{HH} = 2 Hz, OCH₂C≡CH]; 6.52, 6.76, 6.81 [s, 6H, Ar-

H]; 7.00–7.73 [m, 62H, Ar-H, Ph]. Anal. Calcd for C₁₂₄H₁₀₀Au₂Cl₂O₁₆P₄: C, 61.17; H, 4.14. Found: C, 60.71; H, 4.02.

[Resorcinarene(OC(O)OCH₂C≡CH)₄(OPPh₂{AuBr})₂], 11b. This was prepared similarly from **6b** (0.0384 g, 0.0124 mmol) and **1** (0.0246 g, 0.0125 mmol) to produce a white solid. Yield: 0.042 g, 67.1%. NMR [CD₂Cl₂; δ(¹H)]: 1.97, 2.33 [m, 8H, H^j]; 2.46, 2.72 [m, 8H, H^k]; 2.69 [t, 4H, ⁴J_{HH} = 2 Hz, OCH₂C≡CH]; 4.58 [m, 4H, Hⁱ]; 4.76 [m, 8H, ⁴J_{HH} = 2 Hz, OCH₂C≡CH]; 6.51 [s, 2H, H^d]; 6.68 [s, 2H, H^e]; 6.96 [s, 2H, H^a]; 7.00–7.75 [m, 62H, H^b, Ph]. NMR [CD₂Cl₂; δ(¹³C)]: 34.35 [C^k]; 36.56 [C^j]; 36.73 [Cⁱ]; 56.33 [OC(O)OCH₂C≡CH]; 76.53, 76.76 [OC(O)OCH₂C≡CH]; 114.51 [m, C^e]; 114.94 [C^a]; 126.29–134.58 [Ar-C, Ph]; 126.36 [C^d]; 128.45 [C^g]; 129.21 [C^h]; 133.89 [C^c]; 140.81 [ipso-C, CHCH₂-CH₂Ph]; 146.46 [C^b]; 151.95 [C^f]; 152.12 [OC(O)OCH₂C≡CH]. Anal. Calcd for C₁₂₄H₁₀₀Au₂Br₂O₁₆P₄: C, 59.01; H, 3.99. Found: C, 58.58; H, 3.87.

[Resorcinarene(OC(O)OCH₂C≡CH)₄(OPPh₂{AuI})₂], 11c. This was prepared similarly from **6c** (0.0520 g, 0.0179 mmol) and **1** (0.0353 g, 0.0179 mmol) to produce a white solid. Yield: 0.047 g, 53.4%. NMR [CD₂Cl₂; δ(¹H)]: 2.00, 2.37 [m, 8H, H^j]; 2.57, 2.80 [m, 8H, H^k]; 2.64 [t, 4H, ⁴J_{HH} = 2 Hz, OCH₂C≡CH]; 4.61 [m, 4H, Hⁱ]; 4.79 [m, 8H, ⁴J_{HH} = 2 Hz, OCH₂C≡CH]; 6.30, 6.59 [s, 4H, Ar-H]; 6.92–7.74 [m, 64H, Ar-H, Ph]. Anal. Calcd for **11c**•0.5CH₂Cl₂, C_{124.5}H₁₀₁Au₂ClI₂O₁₆P₄: C, 56.21; H, 3.83. Found: C, 56.41; H, 3.52.

[Resorcinarene(OC(O)OCH₂Ph)₄(OPPh₂{AuCl})₂], 12a. This was prepared similarly from **7a** (0.0431 g, 0.0139 mmol) and **2** (0.0303 g, 0.0139 mmol) to produce a white solid. Yield: 0.051 g, 69.4%. NMR [CD₂Cl₂; δ(¹H)]: 2.01, 2.27 [m, 8H, H^j]; 2.39, 2.66 [m, 8H, H^k]; 4.58 [m, 4H, Hⁱ]; 5.15 [s, 8H, OCH₂Ph]; 6.52, 6.71, 6.86 [s, 6H, Ar-H]; 6.90–7.71 [m, 82H, Ar-H, Ph]. Anal. Calcd for **12a**•0.5CH₂Cl₂, C_{140.5}H₁₁₇Au₂Cl₃O₁₆P₄: C, 62.84; H, 4.39. Found: C, 63.16; H, 4.70.

[Resorcinarene(OC(O)OCH₂Ph)₄(OPPh₂{AuBr})₂], 12b. This was prepared similarly from **7b** (0.0330 g, 0.0100 mmol) and **2** (0.0219 g, 0.0101 mmol) to produce a white solid. Yield: 0.048 g, 87.8%. NMR [CD₂Cl₂; δ(¹H)]: 1.98, 2.27 [m, 8H, H^j]; 2.42, 2.66 [m, 8H, H^k]; 4.58 [m, 4H, Hⁱ]; 5.19 [s, 8H, OCH₂Ph]; 6.47 [s, 2H, H^d]; 6.63 [s, 2H, H^e]; 6.87–7.72 [m, 84H, H^a, H^b, Ph]. NMR [CD₂Cl₂; δ(¹³C)]: 34.43 [C^k]; 36.72 [C^j]; 36.80 [Cⁱ]; 70.81 [OC(O)-OCH₂Ph]; 114.03 [m, C^e]; 115.24 [C^a] 126.17 [C^d]; 128.45 [C^g]; 128.53–132.72 [Ar-C, Ph]; 129.12 [C^h]; 133.68 [C^c]; 134.90 [ipso-C, OCH₂Ph]; 140.83 [ipso-C, CH₂CH₂Ph]; 146.67 [C^b]; 151.89 [C^f]; 152.73 [OC(O)OCH₂Ph]. Anal. Calcd for C₁₄₀H₁₁₆Au₂Br₂O₁₆P₄: C, 61.55; H, 4.28. Found: C, 61.16; H, 4.03.

[Resorcinarene(OC(O)OCH₂Ph)₄(OPPh₂{AuI})₂], 12c. This was prepared similarly from **7c** (0.0773 g, 0.0223 mmol) and **2** (0.0485 g, 0.0223 mmol) to produce a white solid. Yield: 0.089 g, 70.6%. NMR [CD₂Cl₂; δ(¹H)]: 2.02, 2.33 [m, 8H, H^j]; 2.51, 2.72 [m, 8H, H^k]; 4.62 [m, 4H, Hⁱ]; 5.23 [s, 8H, OCH₂Ph]; 6.27, 6.55 [s, 4H, Ar-H]; 6.88–7.71 [m, 84H, Ar-H, Ph]. Anal. Calcd for **12c**•0.5*n*-pentane, C_{142.5}H₁₂₂Au₂I₂O₁₆P₄: C, 59.80; H, 4.30. Found: C, 60.02; H, 4.32.

[Resorcinarene(OC(O)C₆H₁₁)₄(OPPh₂{AuCl})₂], 13a. This was prepared similarly from **8a** (0.0750 g, 0.0249 mmol) and **3** (0.0519 g, 0.0249 mmol) to produce a white solid. Yield: 0.092 g, 72.5%. NMR [CD₂Cl₂; δ(¹H)]: 1.05–2.12 [m, 48H, Hⁱ, C₆H₁₁]; 2.27 [m, 4H, H^j]; 2.39, 2.66 [m, 8H, H^k]; 4.53 [m, 4H, Hⁱ]; 6.27, 6.57, 6.92 [s, 6H, Ar-H]; 6.96–7.73 [m, 62H, Ar-H, Ph]. Anal. Calcd for C₁₃₆H₁₃₂Au₂Cl₂O₁₂P₄: C, 64.13; H, 5.22. Found: C, 63.79; H, 5.12.

[Resorcinarene(OC(O)C₆H₁₁)₄(OPPh₂{AuBr})₂], 13b. This was prepared similarly from **8b** (0.0700 g, 0.0219 mmol) and **3**

Table 11. Crystallographic Data for Complexes **6a**, **6c**·THF, **6c**·CH₂Cl₂, and **7c**

	6a	6c ·THF	6c ·CH ₂ Cl ₂	7c
formula	C _{125.2} H _{102.4} Au ₄ Cl _{6.4} O _{16.50} P ₄	C ₁₃₄ H ₁₂₀ Au ₄ I ₄ O _{18.50} P ₄	C ₁₂₉ H ₁₁₁ Au ₄ Cl ₄ I ₄ O ₁₈ P ₄	C ₁₄₂ H ₁₂₀ Au ₄ I ₄ O _{16.50} P ₄
fw	3009.50	3445.65	3510.32	3509.73
space group	<i>P</i> 2 ₁ / <i>n</i>	<i>C</i> 2/ <i>c</i>	<i>C</i> 2/ <i>c</i>	<i>P</i> 2 ₁ / <i>c</i>
<i>a</i> (Å)	18.9439(1)	33.5931(3)	31.371 (2)	21.7191(1)
<i>b</i> (Å)	17.5826(1)	19.1029(2)	19.664(2)	17.8840(1)
<i>c</i> (Å)	36.7552(3)	23.0736(2)	22.756(2)	35.1367(2)
β (deg)	91.496(1)	91.797(1)	94.588(7)	98.847(1)
<i>V</i> (Å ³)	12238.4(1)	14799.6(2)	14037(2)	13485.6(1)
<i>Z</i>	4	4	4	4
<i>D</i> _{calc} (Mg/m ³)	1.633	1.546	1.661	1.729
μ	5.034	4.886	5.226	5.363
R1, wR2 [<i>I</i> > 2σ(<i>I</i>)]	0.0566, 0.1563	0.0436, 0.1226	0.0792, 0.2072	0.0470, 0.1319
R indices (all data)	0.0947, 0.1759	0.0748, 0.1367	0.1400, 0.2496	0.0746, 0.1471

(0.0457 g, 0.0219 mmol) to produce a white solid. Yield: 0.089 g, 76.9%. NMR [CD₂Cl₂; δ(¹H)]: 1.11–1.99 [m, 48H, *H*ⁱ, C₆H₁₁]; 2.32 [m, 4H, *H*^j]; 2.43, 2.69 [m, 8H, *H*^k]; 4.56 [m, 4H, *H*^l]; 6.56 [s, 2H, *H*^a]; 6.58 [s, 2H, *H*^d]; 6.76 [s, 2H, *H*^e]; 6.97–7.73 [m, 62H, *H*^b, *Ph*]. NMR [CD₂Cl₂; δ(¹³C)]: 25.75, 25.81, 26.02, 29.13, 29.24, 42.95 [C₆H₁₁]; 34.69 [C^k]; 36.57 [C^l]; 37.11 [Cⁱ]; 114.56 [m, C^e]; 117.70 [C^a]; 126.28 [C^d]; 128.49–132.80 [Ar-C, *Ph*]; 128.65 [C^e]; 129.65 [C^b]; 134.01 [C^c]; 141.03 [ipso-C, *Ph*]; 146.73 [C^b]; 152.06 [C^l]; 173.97 [C=O].

[Resorcinarene(OC(O)C₆H₁₁)₄{OPPh₂}₂{AuI}]₂, **13c.** This was prepared similarly from **8c** (0.0700 g, 0.0207 mmol) and **3** (0.0432 g, 0.0207 mmol) to produce a white solid. Yield: 0.100 g, 88.5%. NMR [CD₂Cl₂; δ(¹H)]: 1.16–2.08 [m, 48H, *H*ⁱ, C₆H₁₁]; 2.37 [m, 4H, *H*^j]; 2.53, 2.76 [m, 8H, *H*^k]; 4.60 [m, 4H, *H*^l]; 6.36 [s, *H*^d]; 6.69 [s, 2H, *H*^e]; 6.76 [s, 2H, *H*^a]; 6.86–7.77 [m, 62H, *H*^b, *Ph*]. NMR [CD₂Cl₂; δ(¹³C)]: 25.64, 25.84, 26.01, 29.10, 29.35, 43.19 [C₆H₁₁]; 34.76 [C^k]; 35.75 [C^l]; 37.25 [Cⁱ]; 110.47 [m, C^e]; 117.23 [C^a]; 126.28 [C^d]; 126.45–132.75 [Ar-C, *Ph*]; 127.06 [C^e]; 129.22 [C^b]; 134.25 [C^c]; 141.16 [ipso-C, *Ph*]; 146.79 [C^b]; 151.57 [C^l]; 173.91 [C=O]. Anal. Calcd for C₁₃₆H₁₃₂Au₂I₂O₁₂P₄: C, 59.83; H, 4.87. Found: C, 59.48; H, 5.06.

[Resorcinarene(OC(O)C₆H₄CH₃)₄{OPPh₂}₂{AuCl}]₂, **14a.** This was prepared similarly from **9a** (0.0306 g, 0.0101 mmol) and **4** (0.0213 g, 0.0101 mmol) to produce a white solid. Yield: 0.041 g, 78.7%. NMR [CD₂Cl₂; δ(¹H)]: 2.19 [m, 4H, *H*^j]; 2.31 [m, 8H, *H*ⁱ, *H*^k]; 2.50 [s, 12H, C₆H₄CH₃]; 2.63 [m, 4H, *H*^k]; 4.72 [m, 4H, *H*^l]; 6.63 [s, 2H, Ar-*H*]; 6.74–7.78 [m, 82H, Ar-*H*, *Ph*, C₆H₄CH₃]. Anal. Calcd for C₁₄₀H₁₁₆Au₂Cl₂O₁₂P₄: C, 65.20; H, 4.53. Found: C, 64.86; H, 4.15.

[Resorcinarene(OC(O)C₆H₄CH₃)₄{OPPh₂}₂{AuBr}]₂, **14b.** This was prepared similarly from **9b** (0.0578 g, 0.0179 mmol) and **4** (0.0379 g, 0.0179 mmol) to produce a white solid. Yield: 0.072 g, 75.4%. NMR [CD₂Cl₂; δ(¹H)]: 2.12 [m, 4H, *H*^j]; 2.37 [m, 8H, *H*ⁱ, *H*^k]; 2.47 [s, 12H, C₆H₄CH₃]; 2.62 [m, 4H, *H*^k]; 4.75 [m, 4H, *H*^l]; 6.67 [s, 2H, Ar-*H*]; 6.69–7.79 [m, 80H, Ar-*H*, *Ph*, C₆H₄CH₃]. ES-MS: *m/z* 1254 (100%) [M – 2Br]²⁺; *m/z* 2588 (85%) [M – Br]⁺. Anal. Calcd for C₁₄₀H₁₁₆Au₂Br₂O₁₂P₄: C, 63.02; H, 4.38. Found: C, 62.64; H, 3.99.

[Resorcinarene(OC(O)C₆H₄CH₃)₄{OPPh₂}₂{AuI}]₂, **14c.** This was prepared similarly from **9c** (0.0401 g, 0.0118 mmol) and **4** (0.0249 g, 0.0118 mmol) to produce a white solid. Yield: 0.048 g, 73.6%. NMR [CD₂Cl₂; δ(¹H)]: 2.11 [m, 4H, *H*^j]; 2.45 [m, 20H, *H*ⁱ, *H*^k, C₆H₄CH₃]; 2.70 [m, 4H, *H*^k]; 4.75 [m, 4H, *H*^l]; 6.47 [s, 2H, Ar-*H*]; 6.68–7.79 [m, 80H, Ar-*H*, *Ph*, C₆H₄CH₃]. Anal. Calcd for C₁₄₀H₁₁₆Au₂I₂O₁₂P₄: C, 60.88; H, 4.23. Found: C, 61.28; H, 4.44.

[Resorcinarene(OC(O)C₄H₃S)₄{OPPh₂}₂{AuCl}]₂, **15a.** This was prepared similarly from **10a** (0.0550 g, 0.0183 mmol) and **5** (0.0380 g, 0.0183 mmol) to produce a white solid. Yield: 0.071 g, 76.2%. NMR [CD₂Cl₂; δ(¹H)]: 2.17, 2.33 [m, 8H, *H*^j]; 2.42, 2.60

[m, 8H, *H*^k]; 4.76 [m, 4H, *H*^l]; 6.63 [s, 2H, Ar-*H*]; 6.81–7.80 [m, 78H, Ar-*H*, *Ph*, C₄H₃S]. Anal. Calcd for C₁₂₈H₁₀₀O₁₂Au₂Cl₂P₄S₄: C, 60.36; H, 3.96. Found: C, 60.08; H, 3.78.

[Resorcinarene(OC(O)C₄H₃S)₄{OPPh₂}₂{AuBr}]₂, **15b.** This was prepared similarly from **10b** (0.0503 g, 0.0158 mmol) and **5** (0.0329 g, 0.0158 mmol) to produce a white solid. Yield: 0.066 g, 79.2%. NMR [CD₂Cl₂; δ(¹H)]: 2.11, 2.37 [m, 8H, *H*^j]; 2.48, 2.65 [m, 8H, *H*^k]; 4.79 [m, 4H, *H*^l]; 6.65 [s, 2H, Ar-*H*]; 6.76–7.79 [m, 78H, Ar-*H*, *Ph*, C₄H₃S]. Anal. Calcd for C₁₂₈H₁₀₀Au₂Br₂O₁₂P₄S₄: C, 58.32; H, 3.82. Found: C, 57.95; H, 3.69.

X-ray Structure Determinations. Crystals were mounted on glass fibers, and data were collected at 200 K using a Nonius-Kappa CCD diffractometer with Mo Kα (λ = 0.710 73 Å) radiation, using COLLECT (Nonius, BV, 1998) software. The unit cell parameters were calculated and refined from the full data set. Crystal cell refinement and data reduction was carried out using the Nonius DENZO package, and data were scaled using SCALEPACK (Nonius, BV, 1998). The SHELX-TL V5.1 and SHELX-TL V6.1 (G. M. Sheldrick) program packages were used to solve and refine the structures. The structures were solved by direct methods except for **6c**·CH₂Cl₂, **8c**, and **10c**, which were solved using the automated Patterson routine of the SHELX-TL software package. For complexes **6c**·THF, **6c**·CH₂Cl₂, **8a**–**c**, and **10b** the space group could not be unambiguously assigned from the systematic absences. In each case, the centrosymmetric space group *C*2/*c* was chosen on the basis of *E*-statistics and resulted in successful refinement of the data. The hydrogen atoms were calculated geometrically and were riding on their respective carbon atoms. All non-hydrogen atoms were refined with anisotropic thermal parameters unless specified otherwise. All thermal ellipsoid diagrams are shown at 30% probability. Crystal data are summarized in Tables 11–13.

The idealized positions of dummy atoms X were calculated geometrically, assuming linear P–Au–X groups with the P and Au atoms in their crystallographically determined positions and with the same Au–X bond distance as determined.

[Resorcinarene(OC(O)OCH₂C≡CH)₄{OPPh₂}₂{AuCl}]₄, **6a.** Crystals of [C₁₂₄H₁₀₀O₁₆P₄Au₄Cl₄]·1.2CH₂Cl₂·0.5H₂O were grown from diffusion of *n*-pentane into a dichloromethane solution. There was disorder in the molecule. One of the phenethyl groups was modeled as two isotropic half-occupancy groups, and another as a 70:30 isotropic mixture with carbon–carbon single bonds fixed at 1.54 Å. One of the propargyl arms was modeled as a 50:50 isotropic mixture. Two other propargyl carbonate groups were modeled as isotropic 70:30 mixtures with fixed carbon–carbon and carbon–oxygen bond lengths. The carbon–chlorine bond lengths of the solvent molecules were fixed at 1.75 Å. The half-occupancy water molecule was modeled as a single isotropic oxygen atom. There was evidence for an additional disordered partial occupancy solvent molecule, but no suitable model could be refined. The largest

Table 12. Crystallographic Data for Complexes **8a–c** and **9a**

	8a	8b	8c	9a
formula	C ₁₄₉ H ₁₆₀ Au ₄ Cl ₄ O ₁₄ P ₄	C ₁₄₄ H ₁₄₄ Au ₄ Br ₄ N ₄ O ₁₂ P ₄	C ₁₄₃ H ₁₄₇ Au ₄ Cl ₃ I ₄ O ₁₂ P ₄	C ₁₅₈ H ₁₅₂ Au ₄ Cl ₄ I ₄ O _{16.50} P ₄
fw	3228.32	3354.02	3583.30	3368.34
space Group	C2/c	C2/c	C2/c	P1
<i>a</i> (Å)	30.1423(2)	30.5661(3)	30.2786(2)	20.3905(3)
<i>b</i> (Å)	16.1005(1)	16.2604(2)	16.4113(1)	21.5794(3)
<i>c</i> (Å)	31.6305(3)	31.4572(3)	31.8044(3)	22.8535(5)
α (deg)				101.783(1)
β (deg)	117.001(1)	117.285(1)	116.399(1)	110.963(1)
γ (deg)				111.272(1)
<i>V</i> (Å ³)	13677.3(2)	13903.1(3)	14155.9(2)	8080.3(2)
<i>Z</i>	4	4	4	2
<i>D</i> _{calc} (Mg/m ³)	1.568	1.602	1.681	1.384
μ	4.463	5.462	5.163	3.782
R1, wR2 [<i>I</i> > 2 σ (<i>I</i>)]	0.0418, 0.0930	0.0579, 0.1644	0.0644, 0.1825	0.0803, 0.2107
R indices (all data)	0.0734, 0.1038	0.1003, 0.1936	0.0901, 0.2033	0.1493, 0.2477

Table 13. Crystallographic Data for Complexes **10a–c**

	10a	10b	10c
formula	C _{131.50} H _{103.50} Au ₄ Cl _{14.50} O ₁₂ P ₄ S ₄	C ₁₄₆ H ₁₃₆ Au ₄ Br ₄ O _{16.50} P ₄ S ₄	C ₁₃₂ H ₁₀₄ Au ₄ Cl ₁₂ I ₄ O ₁₂ P ₄ S ₄
fw	3429.65	3514.17	3855.14
space group	P1	C2/c	P1
<i>a</i> (Å)	18.0604(2)	39.2913(3)	17.3538(1)
<i>b</i> (Å)	19.4505(2)	17.4399(1)	20.1204(2)
<i>c</i> (Å)	22.7859(3)	24.9380(2)	23.7107(2)
α (deg)	72.693(1)		70.341(1)
β (deg)	68.422(1)	114.729(1)	68.580(1)
γ (deg)	70.800(1)		70.711(1)
<i>V</i> (Å ³)	6885.8(1)	15521.4(2)	7051.7(1)
<i>Z</i>	2	4	2
<i>D</i> _{calc} (Mg/m ³)	1.654	1.504	1.816
μ	4.693	4.950	5.411
R1, wR2 [<i>I</i> > 2 σ (<i>I</i>)]	0.0469, 0.1262	0.0506, 0.1626	0.0504, 0.1294
R indices (all data)	0.0680, 0.1428	0.0743, 0.1790	0.0878, 0.1490

residual electron density peak (3.582 e/Å³) was associated with one of the solvent molecules.

[Resorcinarene(OC(O)OCH₂C≡CH)₄(OPPh₂{AuI})₄]₄, 6c·THF. Crystals of [C₁₂₄H₁₀₀Au₄I₄O₁₆P₄]₄·2.5THF were grown from diffusion of *n*-hexane into a THF solution. Two of the partial occupancy THF molecules were modeled isotropically with carbon–oxygen and carbon–carbon bond lengths fixed. The largest residual electron density peak (1.497 e/Å³) was associated with one of the iodine atoms (I2).

[Resorcinarene(OC(O)OCH₂C≡CH)₄(OPPh₂{AuI})₄]₄, 6c·CH₂Cl₂. Crystals of [C₁₂₄H₁₀₀Au₄I₄O₁₆P₄]₄·(2CH₂Cl₂)·0.5*n*-hexane·2H₂O were grown from diffusion of *n*-hexane into a dichloromethane solution. One of the dichloromethane molecules was modeled with fixed carbon–chlorine bond lengths, and the *n*-hexane was modeled with fixed carbon–carbon distances. The adventitious water was modeled as an isotropic oxygen atom. The crystal lost solvent during data collection, even at low temperature, and so an incomplete data set was obtained. Only the gold, iodine, and phosphorus atoms could be refined with anisotropic thermal parameters. The largest residual electron density peak (1.768 e/Å³) was associated with one of the carbon atoms (C300).

[Resorcinarene(OC(O)OCH₂Ph)₄(OPPh₂{AuI})₄]₄, 7c. Crystals of [C₁₄₀H₁₁₆Au₄I₄O₁₆P₄]₄·0.5THF were grown from diffusion of methanol into a THF solution. Two of the carbonyl groups (C12B–O5B and C10B–O2B) were modeled as a mixture of two isotropic half-occupancy groups. One of the phenyl rings (C2C1–C2C6) attached to phosphorus P3 was modeled as an isotropic 60:40 disorder. The half-occupancy THF was poorly behaved and was modeled isotropically with carbon–carbon and carbon–oxygen distances fixed. The largest residual electron density peak (2.716 e/Å³) was associated with one of the iodine atoms (I4).

[Resorcinarene(OC(O)C₆H₁₁)₄(OPPh₂{AuCl})₄]₄, 8a. Crystals of [C₁₃₆H₁₃₂Au₄Cl₄O₁₂P₄]₄·2THF·*n*-pentane were grown from diffusion of *n*-pentane into a THF solution. The phenethyl groups were modeled as a mixture of two isotropic half-occupancy groups. One of the carbonyl moieties of the cyclohexylcarboxylate substituents was modeled as a mixture of two isotropic half-occupancy groups. The *n*-pentane and one THF were modeled as two isotropic half-occupancy groups, with geometrical constraints. The largest residual electron density peak (1.268 e/Å³) was associated with one of the oxygen atoms (O2B).

[Resorcinarene(OC(O)C₆H₁₁)₄(OPPh₂{AuBr})₄]₄, 8b. Crystals of [C₁₃₆H₁₃₂Au₄Br₄O₁₂P₄]₄·4CH₃CN were grown from diffusion of acetonitrile into a chloroform solution. One of the phenyl rings was modeled as a mixture of two isotropic half-occupancy groups, and one phenethyl group was modeled as a mixture of two isotropic half-occupancy groups. One of the carbonyl moieties of the cyclohexylcarboxylate substituents was also modeled as a mixture of two isotropic half-occupancy groups. One of the acetonitrile molecules was disordered across a symmetry element and was modeled as an isotropic 50:50 mixture. The largest residual electron density peak (1.872 e/Å³) was associated with one of the gold atoms (Au1).

[Resorcinarene(OC(O)C₆H₁₁)₄(OPPh₂{AuI})₄]₄, 8c. Crystals of [C₁₃₆H₁₃₂Au₄I₄O₁₂P₄]₄·CHCl₃·*n*-hexane were grown from diffusion of *n*-hexane into a chloroform solution. The chloroform was disordered across a symmetry element and was modeled as a 50:50 isotropic disorder of the carbon atoms with fixed carbon–chlorine bond lengths, and the *n*-hexane was modeled with fixed carbon–carbon distances. The largest residual electron density peak (2.972 e/Å³) was associated with one of the gold atoms (Au2).

[Resorcinarene(OC(O)C₆H₄CH₃)₄(OPPh₂{AuCl})₄], 9a. Crystals of [C₁₄₀H₁₁₆Au₄Cl₄O₁₂P₄] \cdot 4.5THF were grown from diffusion of *n*-hexane into a THF solution. The compound was well ordered, whereas the solvents of crystallization were not and were treated with geometrical constraints. The solvents of crystallization and the phenyl rings of the diphenylphosphinite groups were refined isotropically. The largest residual electron density peak (1.795 e/Å³) was associated with one of the gold atoms (Au3).

[Resorcinarene(OC(O)C₄H₃S)₄(OPPh₂{AuCl})₄], 10a. Crystals of [C₁₂₈H₁₀₀Au₄Cl₄O₁₂P₄S₄] \cdot 3.5CHCl₃ were grown from diffusion of *n*-hexane into a chloroform solution. The solvent molecules were disordered, as was one of the thiophene groups. The largest residual electron density peak (2.424 e/Å³) was associated with one of the gold atoms (Au1).

[Resorcinarene(OC(O)C₄H₃S)₄(OPPh₂{AuBr})₄], 10b. Crystals of [C₁₂₈H₁₀₀Au₄Br₄O₁₂P₄S₄] \cdot 4.5THF were grown from diffusion of *n*-hexane into a THF solution. A disordered thiophene was modeled after the well-ordered thiophene group and by comparison with literature data.¹⁵ The disorder was modeled as a 50:50 mixture of isotropic thiophene rings, rotated about a C₂ axis bisecting the thiophene ring along C10B. A phenyl group was modeled as a 50:

50 mixture of two isotropic rings. The largest residual electron density peak (2.939 e/Å³) was not associated with any atom.

[Resorcinarene(OC(O)C₄H₃S)₄(OPPh₂{AuI})₄], 10c. Crystals of [C₁₂₈H₁₀₀Au₄I₄O₁₂P₄S₄] \cdot 4CHCl₃ were grown from diffusion of *n*-hexane into a chloroform solution. There was disorder in three of the thiophene groups, and they were modeled after the one well-ordered thiophene group and by comparison with literature data.¹⁵ The disorder was modeled as a 50:50 mixture of isotropic thiophene rings, rotated about a C₂ axis bisecting the thiophene ring along C10B (C10D, C15B). The largest residual electron density peak (2.046 e/Å³) was associated with one of the iodine atoms (I4).

Acknowledgment. We thank the NSERC (Canada) for financial support. R.J.P. thanks the Government of Canada for a Canada Research Chair.

Supporting Information Available: Crystallographic tables in CIF format for complexes **6a**, **6c** \cdot THF, **6c** \cdot CH₂Cl₂, **7c**, **8a–c**, **9a**, and **10a–c**. This material is available free of charge via the Internet at <http://pubs.acs.org>.

IC034430C